NACA TN 3248

NATIONAL ADVISORY COMMITTEE FOR AERONAUTICS

TECHNICAL NOTE 3248

AN EXPERIMENTAL AND THEORETICAL INVESTIGATION OF THE ANISOTROPY OF 3S ALUMINUM-ALLOY SHEET IN THE PLASTIC RANGE

By Arthur J. McEvily, Jr., and Philip J. Hughes

Langley Aeronautical Laboratory
Langley Field, Va.

Washington
October 1954

NATIONAL ADVISORY COMMITTEE FOR AERONAUTICS

TECHNICAL NOTE 3248

AN EXPERIMENTAL AND THEORETICAL INVESTIGATION OF THE ANISOTROPY OF 3S ALUMINUM-ALLOY SHEET IN THE PLASTIC RANGE

By Arthur J. McEvily, Jr., and Philip J. Hughes

SUMMARY

The results of tension and compression tests on 3S aluminum-alloy sheet are presented together with values of Poisson's ratio in the plastic range. Crystallographic anisotropy was found to be responsible for the variation in Poisson's ratio in the width and thickness directions of specimens alined at various angles with respect to the rolling direction in the plane of the sheet. X-ray diffraction studies of annealed specimens were made and pole figures showing the type of preferred orientation were drawn. A theoretical analysis was made to account for the observed anisotropy based on the behavior of single crystals and on the texture of the sheet. An independent check of the theory is afforded through comparison with experimental data on cubically alined copper sheet.

INTRODUCTION

All metals are anisotropic to some extent. In the elastic range, the effect of this anisotropy on the mechanical properties is usually negligible. In particular, aluminum alloys are usually isotropic in the elastic range. In the plastic range, however, anisotropic effects may be highly pronounced.

Klingler and Sachs (refs. 1 to 3) have listed three distinct types of anisotropy: anelastic, mechanical, and crystallographic. Anelastic anisotropy is caused by the residual stresses resulting from the cold-working of the material. Mechanical anisotropy is due to the geometrically directional arrangement of certain phases, inclusions, porosities, cracks, and similar factors. Crystallographic anisotropy is caused by the preferential orientation of the grains making up the polycrystalline aggregate, the grains being inherently anisotropic because of the nature of their crystalline structure.

The present paper is concerned with (1) an experimental investigation of the extent and type of anisotropy present in an annealed aluminum-alloy sheet material, and (2) a theoretical analysis to account quantitatively for the observed anisotropy. Tension and compression stress-strain tests were made on specimens cut from sheets of 3S aluminum alloy at various angles with respect to the rolling direction. The values of Poisson's ratio, a sensitive index of anisotropy, were determined for the width and thickness directions of the tension specimens in both the elastic and plastic ranges. In addition, microscopic and crystallographic examinations of the material were made in order to gain information concerning the types of anisotropy present.

The theoretical analysis to account for the anisotropy was made on the basis of the properties of single crystals and on the preferred grain orientation deduced from the crystallographic studies.

SYMBOLS

ϵ	plastic strain
μ	Poisson's ratio in plastic range
I	intensity of reflected X-ray beam
L	longitudinal axis of tension specimen
X,Y	arbitrary orthogonal directions in cross section of specimen
γ	shear strain
l	direction cosine
λ	angle between normal to slip plane and specimen axis
β	angle between slip direction and specimen axis
φ	angle between slip direction and projection of specimen axis on slip plane
α	angle of rotation in cross section from line of interception of slip plane with cross section to direction of maximum strain

Subscripts:

t	thickness direction of tension specimen
w	width direction of tension specimen

mn tensor notation

hkl Miller indices which designate a set of parallel planes (hkl) from which X-ray beam β is reflected

Numerical subscripts refer to axes given in figure 20.

STRESS-STRAIN TESTS

Materials and Specimens

The specimens used in the stress-strain tests were machined from three 1/8-inch-thick sheets of 3S aluminum alloy. The sheets were obtained in the -H14 condition (formerly designated as -1/2 Hard). The nominal composition of this alloy is 1.2 percent manganese and the rest aluminum and normal impurities (ref. 4). (3S is essentially commercially pure aluminum with the addition of a small amount of manganese.) Photomicrographs of this material in the annealed condition, taken on various planes, are presented in figure 1.

Although the exact processing history of these sheets is unknown, a description of a typical manufacturing procedure for such material may be pertinent. The usual procedure is to roll a sheet of this type from an ingot 10 inches thick, the ingot receiving reversals between rolling passes in the early stages of hot-rolling. When reduced to a thickness of 0.215 inch, the sheet receives a process anneal at 800° F. The material is then cold-rolled to 0.125 inch thick. This treatment amounts to a reduction after annealing of approximately 42 percent and brings the material to the -H14 condition.

In order to permit the study of a known amount of cold-work upon the behavior of the material, two of the sheets were annealed at 750° F for 1 hour and then strained in tension parallel to the rolling direction. One sheet was strained 1 percent; the other, 5 percent. After the material had been treated in this manner, a series of standard tension and compression specimens were machined from each of these two sheets at various angles with respect to the rolling direction. The layout and dimensions of these specimens are shown in figure 2. At least two specimens were tested for each orientation.

A similar series of specimens was prepared from the third sheet. These specimens were tested in the annealed condition without prestrain. Because the material in the annealed condition was extremely soft, specimens were machined from the sheet before annealing in order to minimize effects associated with the machining process.

Tests

The tension and compression tests were performed in a hydraulic testing machine operated at a constant strain rate of approximately 0.002 in./in./min. The stress-strain curves were drawn autographically with a maximum inaccuracy of ±2 percent. The compression specimens were supported in a grooved-plate type of supporting fixture (ref. 5). Strains were measured along both edges with a pair of variable differential transformer extensometers. The range of the compression tests was limited by contact between the loading head and the supporting fixture. The tension specimens were held by Templin grips. Again the stress-strain curves were autographically recorded, but additional strains were measured in the width and thickness directions for the purpose of determining the values of Poisson's ratio. These lateral strains were measured with special gages, shown in figure 3, placed within the longitudinal-gage length. The tension setup is shown in figure 4, the longitudinal gages being omitted for clarity. The tension tests were carried to the limit of the recorder, at which point the gages were removed. The tests were then continued until failure occurred.

Test Results

Stress-strain curves.- The stress-strain curves for tension and compression are presented in figures 5 and 6, respectively. These curves were obtained by averaging the curves of at least two specimens for each orientation. When the results are presented, only the tests for the rolling and transverse directions (0° and 90°) are shown because all the curves for a given prestrain value lie in a narrow region. For the specimens with 1 and 5 percent prestrain, the tension curves are progressively lower as the specimen axis moves toward the transverse axis of the sheet, whereas in compression the reverse is true. For the specimens without prestrain, the stress-strain curves for the various orientations are grouped in such close proximity that the difference between curves is not significant. Values of yield strength (0.2 percent offset) and ultimate tensile strength for the annealed and the prestrained specimens are presented in table 1.

Poisson's ratio.- The average values of Poisson's ratio obtained in the tension tests are presented in figures 7 to 11. The values of Poisson's ratio were obtained by dividing the negative value of the lateral strain ϵ_t or ϵ_w by the corresponding longitudinal strain ϵ_L. Poisson's ratio for the thickness direction μ_t is then given by $-\epsilon_t/\epsilon_L$, and Poisson's ratio for the width direction μ_w is given by $-\epsilon_w/\epsilon_L$. Values for both μ_t and μ_w were about 0.3 in the elastic range, and, as is shown in figures 7 to 11, in the plastic range the value of μ_t

was approximately 0.6 in the thickness direction; whereas the value of μ_w was about 0.4 for plastic strains of 3 percent.

Discussion of Results

The stress-strain curves for the annealed material are located in such close proximity that they reveal little concerning the presence of anisotropy. The Poisson's ratio curves, however, very definitely show that anisotropy is present not only in the prestrained material but also in the annealed material. Because of this clearly defined anisotropy, an effort was made to determine which type or types of anisotropy were responsible for the observed behavior. The evidence for or against the presence of each type of anisotropy is presented subsequently.

Anelastic anisotropy.- The presence or absence of this type of anisotropy can best be detected from the stress-strain curves. Examination of figures 5 and 6 and of table 1 reveals a systematic variation of yield strength with orientation for the prestrained material, both in tension and in compression. For the annealed material, however, these differences are much smaller and if there is any trend at all present, it appears to be in a direction opposite to that of the prestrained material. It is considered that the annealing of the 3S-H14 material has removed the residual stresses due to the rolling process. Subsequent prestraining introduces residual stresses which bring about the type of anelastic anisotropy observed in the prestrained sheets. The annealed material, however, is free of anelastic anisotropy.

Note that the anisotropy introduced by prestraining is the same for a 5 percent prestrain as for a 1 percent prestrain; this similarity suggests that there is a limit to the amount of anelastic anisotropy that can be developed in a material. This result is in accord with the findings of Klingler and Sachs (ref. 1), who state that, for 24S-T aluminum alloy, the Bauschinger effect remains approximately constant for prestrains exceeding 1 or 2 percent. They also found that the anisotropy of 24S-T aluminum in compression after prestretching is considerably smaller than that in tension. Examination of the yield stress values in table 1 shows that the reverse effect is true of the prestretched 3S-O material.

Mechanical anisotropy.- Polished and etched specimens of annealed 3S material were examined under the microscope in order to detect inclusions, cracks, or porosities which might give rise to mechanical anisotropy. Small, randomly scattered inclusions were detected, but no cracks or porosities were noticed. The absence of cracks or porosities and the evident randomness of the inclusions constitute evidence against the presence of any significant degree of mechanical anisotropy.

Crystallographic anisotropy.- For the annealed material, in the absence of anelastic or mechanical anisotropy, it seems highly probable that crystallographic anisotropy must be responsible for the observed variation in Poisson's ratio. For the prestrained material, in addition to the crystallographic anisotropy, anelastic anisotropy has been added because of the prestrain.

In order to substantiate the conclusion that 3S material possessed crystallographic anisotropy, a study of the nature of the texture of the annealed sheet was undertaken, and an attempt was made to correlate the preferred orientation with the experimental results. This program is described in the succeeding sections.

TEXTURE OF 3S-O SHEET

The standard means for describing the preferred orientation or texture of a polycrystalline aggregate is the pole figure. The pole figure is a stereographic projection which indicates the distribution of lattice planes in different orientations. In order to determine this distribution, it is usually necessary to make an X-ray diffraction study of the material. Inasmuch as the intensity of the diffracted beam is proportional to the concentration of lattice planes, an estimate of the relative number of grains of a certain orientation may be made. The accuracy of this estimate can be improved through the use of a Geiger counter spectrometer to measure the intensity of the diffracted beam. The details of the texture studies in the present investigation are presented in appendix A.

The pole figures for the interior of the annealed sheet material determined by X-ray diffraction analysis are presented in figure 12. The textures of the sheet centered about the ideal orientations in table 2. Relative percentages of each type of ideal orientation, as determined in appendix A, are also given.

In table 2, the Miller indices in parentheses indicate the plane in the face-centered cubic aluminum crystal which is parallel to the rolling plane, and the indices in brackets indicate the crystallographic direction which is parallel to the rolling direction. Examination of the pole figure reveals that the oriented grains do not possess exactly the ideal orientations listed previously but center about them. The last item in table 2 (random: 15 percent) indicates that 15 percent of the grains of the aggregate did not center about any particular orientation; instead, their poles were distributed uniformly through all possible orientations.

CALCULATED VALUES OF POISSON'S RATIO

Method of Calculation

Studies of face-centered cubic single crystals at room temperature have established the fact that plastic deformation takes place by slip along the {111} type plane in the <110> type direction for which the resolved shear stress is a maximum. With the aid of a few assumptions, calculations can be made for the values of Poisson's ratio in the plastic range of a polycrystalline metal if the behavior of the aggregate is taken to be the average of the contributions of the individual grains considered as single crystals. When these calculations are made, the longitudinal strain in each grain is assumed to be the same as for the aggregate as a whole, and slip is assumed to take place in all the grains of the aggregate. Then, with information on the orientation of each of the grains, the strain in any direction of the aggregate may be calculated if shearing deformation caused by slip is the only mode of deformation considered.

Inasmuch as the textures of the 3S-O sheet have been established, all the necessary information for determining relative strains in the plastic range is at hand. However, in order to illustrate the method of computation and to assess the validity of the method, a simple case dealing with a single texture is considered before proceeding to the more complex case of the 3S-O aluminum alloy with its several textures.

An Elementary Case: Cubically Alined Copper

A series of tests have been performed by Baldwin, Howald, and Ross (ref. 6) on cubically alined, (001)[100], copper sheet. Lateral strains were measured in the plastic range for specimens cut in the plane of the sheet at various angles with respect to the rolling direction. From the data of reference 6, values of Poisson's ratio in the plastic range have been computed by assuming constant volume and are presented in figure 13.

Klingler and Sachs (ref. 2) have used these data in an attempt to correlate the behavior of single crystals with that of polycrystalline material. As shown in figure 13(a), they compared the data with theoretical values of Poisson's ratio calculated in reference 7 on the basis of a single-crystal model; in addition, they also showed Poisson's ratios obtained experimentally in reference 8 for a single crystal. On the basis of this comparison, Klingler and Sachs concluded that it is impossible, at present, to predict the plastic behavior of a material from a known preferred orientation.

Examination of reference 8, however, reveals that the plastic strains used to calculate Poisson's ratio were taken as the maximum and minimum values of transverse strain in a cylindrical, single-crystal specimen. Similarly, the theoretical calculations of reference 7 are for the maximum and minimum values of Poisson's ratio in the cross section of a stretched crystal. Consequently, the comparison made by Klingler and Sachs with the sheet data of Baldwin, Howald, and Ross appears to be in error because the width and thickness directions of the sheet were not the directions of maximum or minimum strain in the cross section.

Expressions have been derived in appendix B for the relative value of the maximum and minimum strains in the cross section, together with their orientations. The theoretical values of Poisson's ratio obtained through the use of these expressions agree with the theoretical values presented by Klingler and Sachs.

The curve of Poisson's ratio for a (001)[100] ideal orientation (fig. 14) is applicable to the cubically alined copper sheet under discussion. This curve has been obtained by using the method outlined in appendix B. In figure 13(b), this curve is compared with the experimental data of Baldwin, Howald, and Ross (ref. 6). When these theoretical and experimental values for the width and thickness directions of the sheet are compared, a wide discrepancy is noted in the region within 20° of the rolling direction and also of the transverse direction. Examination of the pole figures of Baldwin, Howald, and Ross indicates a spread of approximately 10° about the ideal orientation, (001)[100]. This spread is indicated by the shaded regions of figure 15. In addition, the active slip systems for a face-centered cubic crystal are also shown in this figure. Values of μ_t and μ_w have been calculated which take this spread into account.

Each of the shaded regions was broken into smaller elements, and the specimen axis was assumed to pass through the center of each of these elements. Weighted average values of μ_t and μ_w based on the relative sizes of the elements were then computed. In order to illustrate this method, a discussion of the 10° case is now considered. The shaded region was subdivided into elements as shown in figure 15(b). The specimen axis for each element is related to the ideal axis by rotation about the pole of the great circle through the ideal orientation and the center of the element. This rotation also involves a corresponding shift of the thickness and width axes. The method of computation outlined in appendix B was then employed for each section and the weighted averages were computed. The results of these theoretical computations which consider this spread are shown in figure 13(c) in the form of a curve entitled "present modified theory." The good agreement between this curve and the experimental data for the 10° case is due to the consideration of another slip system associated with region C in figure 15(b).

The success of these calculations in predicting the behavior of a polycrystalline aggregate based on single-crystal properties validated the assumptions and made the attempt to compute similar values for the 3S-0 material seem feasible. The results of these computations will now be described.

Theoretical Values of Poisson's Ratio for 3S-0 Aluminum Alloy

The theoretical calculations for the 3S-0 aluminum alloy are presented in detail in appendix B. Figure 16 shows how the value of Poisson's ratio varies with the angle between the loading and rolling direction (the loading axis is in the rolling plane) for single crystals with ideal orientations corresponding to the ideal orientations present in the 3S-0 sheet. The Poisson's ratio variation for the (100)[001] case has already been shown in figure 14. Only values of μ_w are shown, since μ_t is merely $1 - \mu_w$.

The discontinuities shown in these curves occur at the boundaries of the spherical triangles which determine the active slip system (fig. 15(a)). Whenever the specimen axis moves from one triangle to another, there is a change in slip system, and the resultant plastic deformations associated with this new slip system may be very different from the plastic deformations associated with the previous slip system.

In figure 17, theoretical values for μ_w for any loading direction in the plane of the 3S-0 sheet are presented. These values are the weighted averages of the contributions of each of the ideal orientations taken from figure 16; the weighting factor for each contribution was taken proportional to the percentage of the corresponding ideal orientation determined by the crystallographic analysis.

Figure 17(b) is a curve faired to eliminate the discontinuities of the theoretical curve. Wherever a jump in the theoretical curve occurs, the curve is faired through the midpoint of this transition. The curve also passes through the ends of the pips of the theoretical curve. This curve is used to compare theory with experiment.

Theoretical and experimental values of μ_t and μ_w are compared in figure 18. The experimental values were obtained at a longitudinal strain of 3 percent. This value of strain was selected to insure that all grains had slipped. This selection seems to be reasonable in the light of work by Hedgepeth, Batdorf, and Sanders (ref. 9) who found that all the grains in a 2S-0 tensile specimen had slipped before a 2.2 percent strain.

When these computations were made for the annealed alloy, the elastic contribution to the value of Poisson's ratio was omitted, because its value is only about 2 percent of the total lateral strain at a longitudinal strain of 3 percent.

Discussion of Results

Examination of figure 18 reveals fairly good agreement between theoretical and experimental values in all cases where data were obtained. Inasmuch as good overall agreement exists between theory and experiment, the assumptions made in the analysis appear to be justified. For materials which possess a high degree of preferred orientation, it is expected that the spread of grain orientations about the ideal orientations would be minimized, and agreement between theory and experiment thereby improved. The modification of theoretical values by spread in orientation has not been applied to the 3S-O material except in a general way by fairing the theoretical curve of figure 17. From an examination of figure 17(a), it appears that, even if data on the extent of spread were obtained, the effect of spread on the weighted averages of many ideal orientations would be small in the regions of the curve where experimental values of Poisson's ratio were determined.

Although these computations have been made only for the annealed material, they should also apply fairly well to the prestrained material, because the small prestrains involved would not cause any appreciable change in the texture of the material. Examination of figures 7 to 11 shows that, at the larger values of longitudinal strain, the values of Poisson's ratio for the prestrained material are indeed close to the values for the annealed material.

CONCLUDING REMARKS

The determination of Poisson's ratio of 3S aluminum-alloy sheet in the plastic range has revealed a high degree of anisotropy which has been shown to be essentially crystallographic in nature. The success of the proposed theory in accounting for the observed anisotropy for this material and also for cubically alined copper indicates the feasibility of methods of calculations which are based on the properties of single crystals to account for polycrystalline behavior in the plastic range.

Langley Aeronautical Laboratory,
National Advisory Committee for Aeronautics,
Langley Field, Va., July 20, 1954.

APPENDIX A

DETERMINATION OF PREFERRED ORIENTATION

Pole Figures

A standard method of determining preferred orientation in a metal is to establish the pole figures for the important planes of the material. The pole figures indicate the distribution of the normals to important crystallographic planes in polycrystalline aggregates. A complete description of the general procedure used in the establishment and interpretation of these figures may be found in reference 10. A detailed description of the particular procedures and interpretation for the 3S-O material follows.

In order to obtain the information required to draw the pole figures, a flat specimen was prepared from the interior of the sheet. Light cuts were taken in the machining operation and the last 0.005 inch below the machined surfaces was removed by etching in dilute hydrochloric acid. The final thickness of this specimen was 0.030 inch. In addition, a cylindrical specimen, 0.060 inch in diameter with its axis in the rolling direction, was similarly prepared from the interior of the sheet. These dimensions were selected in order to obtain diffracted beams of maximum intensity. All machining and etching operations were performed on the material in the -H14 condition. The specimens were then annealed for 1 hour at 750° F to correspond to the process anneal of the material used in the stress-strain studies.

Transmission X-ray diffraction patterns were obtained from the specimens utilizing molybdenum Kα radiation. An integrating camera was used because of the large grain size of the annealed material. All diffraction patterns in this phase of the work were recorded on film. The transmission patterns were obtained with the X-ray beam normal to the rolling direction and making angles of 0°, 10°, 15°, 30°, 45°, 60°, 75°, and 90° with the normal to the rolling plane; an additional pattern was obtained with the beam normal to the transverse direction and making an angle of 10° with the normal to the rolling plane. Above 45°, the patterns obtained from the cylindrical specimen were used because the absorption characteristics of this type of specimen do not change when rotated about its longitudinal axis; whereas patterns obtained from flat specimens are difficult to interpret because of extensive absorption at angles above 45°. Below 45°, the patterns obtained from both flat and cylindrical specimens were used. The patterns obtained were then plotted on Wever-type charts. Three degrees of shading were used to represent the different degrees of intensity of the diffraction rings present on the films. The resultant pole figures for the interior octahedral and cubic planes are shown in figure 12.

Examination of these pole figures reveals that the texture of the material is not sharply defined. It is pointed out in reference 10 that a thickness reduction of 90 percent or more may be required before a texture is fully developed and that the general process of reorientation in many cases is not even noted before a reduction of one-third or one-half. Because the material in this study has been reduced only 42 percent after the process anneal and because many grains recrystallize in situ (ref. 11), the lack of sharpness in the figures is not surprising.

In order to treat the information given in the pole figures in a quantitative fashion, the observed texture was assumed to be centered about certain ideal orientations. A search of the literature was made in order to learn which ideal rolling and recrystallization textures had previously been found to describe the preferred orientation of rolled and annealed aluminum sheet. The principal rolling and recrystallization textures, which are applicable to the present data, are the $(110)[1\bar{1}2]$, $(110)[\bar{1}12]$, $(112)[\bar{1}\bar{1}1]$, $(210)[1\bar{2}2]$, $(210)[\bar{1}22]$, $(001)[100]$, $(113)[\bar{2}\bar{1}1]$, and $(113)[\bar{1}\bar{2}1]$ orientations. (For convenience in later calculations, the $(110)[112]$, $(113)[121]$, and $(210)[122]$ orientations have been subdivided into their equally probable twin components.) These ideal orientations have been plotted as points on the pole figures (fig. 12), and describing the observed texture as one which centers about these five types is seen to be reasonable. Other ideal orientations were tried but did not fit the observed data as well, or else they varied only slightly from the previously mentioned components. In addition to these components, the completeness of all diffraction rings indicated that a percentage of randomly oriented grains must also be present.

In addition to the pole figures for the interior of the sheet, a surface specimen was prepared which was 0.005 inch thick. The texture of the surface layers was also studied. Patterns from this specimen were obtained by using copper Kα radiation and indicated that the surface was similar to the interior of the sheet with a trace of the $(100)[110]$ surface texture present.

Quantitative Determination of Texture

Because the texture of the 3S-O aluminum alloy was made up of a number of ideal orientations, a knowledge of the relative amount of each type is necessary before the observed anisotropy can be accounted for. To make such an estimate based on film work alone is difficult. An appropriate method involves the use of a Geiger counter spectrometer together with an automatic chart recorder; this method enables a direct comparison of diffracted beam intensities to be made. For this spectrometer work, copper Kα radiation was used and only those planes parallel to the rolling plane were investigated.

When aluminum, which has a face-centered cubic crystal lattice, is irradiated with copper Kα radiation, the following diffracted beams are obtained: 111, 200, 220, 311, 222, 400, 331, 420, 422, 511, and 333. These indices correspond to the reflecting plane multiplied by the order of reflection. All the planes of ideal orientation parallel to the rolling plane of the listed textures are included in this listing; as will be shown, this fact permits an estimate of the relative percentage of each type present to be made because the concentrations of lattice planes are proportional to the diffracted intensities.

Each of the reflections is considered to be made up of two parts - one being the reflection from planes parallel to the rolling plane and the other being the contribution to the diffraction pattern of the randomly oriented grains. In order to determine this second part, a specimen of fine filings from the -H14 sheet was prepared and annealed. This specimen was considered to possess a random orientation. These filings were mixed with a nitrocellulose binder and placed in a plastic holder which had a shallow recess so that the filings filled a region 1/8 inch deep with a flat surface of 1/2 by 1 inch. The surface of the specimen was set so that it was tangent to the copper Kα beam radiation which then entered the Geiger counter. A fine entrance slit and large exit slit were used to insure that the entire diffracted beam entered the Geiger counter throughout the angular range of measurement. Soller antiscatter slits were also used to reduce the background. The specimen was rotated about an axis in the surface of the specimen which was perpendicular to the incident X-ray beam. The Geiger counter rotated about the same axis through an angle which was twice that of the specimen rotation so that it was always in position to intercept diffracted beams from planes parallel to the surface. The Geiger counter was positioned to receive the maximum intensity of the diffracted beam from a given set of planes and a timed count of the intensity was made. Continuous automatic chart recordings of the variation of diffracted-beam intensity with angle of rotation were also obtained. A typical chart obtained from the filings is shown in figure 19(a). This chart is shown for illustrative purposes only. All calculations were based on the timed-count readings. The 111 reflection, corrected for background, was selected as the basis for comparison and was assigned a value of 1.00. The relative intensities of the reflected beams are given in table 3.

In addition, theoretical values are also listed for the purpose of checking the measured intensity values. The method used in obtaining the theoretical values is described in reference 10. Fortunately, no correction of the theoretical values for an absorption effect was necessary because, for the case of diffraction from planes parallel to the surface of the specimen, the absorption correction is a constant factor independent of the angle of diffraction (ref. 12). Therefore, when the intensities are expressed as ratios, this constant absorption term is

canceled. The agreement between the experimental and theoretical values was considered to be satisfactory. When the values in table 3 were determined, only the experimentally obtained relative intensity values were used.

In a similar manner, counts of the reflected intensities for planes parallel to the rolling plane were determined for specimens prepared from the surface and the interior of the sheet. As in the film work establishing the pole figures, the large grain size of the 3S-O aluminum alloy necessitated the use of an integrating device. Charts typical of the reflections from the interior and surface of the sheet are shown in figures 19(b) and (c), respectively. Again, these charts are presented for illustrative purposes only. A comparison of the measurements of reflected intensities from a lightly etched surface specimen and an interior specimen indicated that the surface textures were essentially the same as the interior textures, the rolling textures being slightly more pronounced in the surface layers.

The assumption was made that the entire 111 reflection was from grains of random orientation, because the rolling or recrystallization textures are not characterized by a (111) plane in the rolling plane. These random grains would affect the other reflections in proportion to the values given in table 3. Each reflection then consisted of two parts, one due to the ideal orientation and the other due to the random component.

Let $(I_{hkl})_{specimen}$ refer to the intensity count due to the (hkl) planes of the 3S-O aluminum alloy. The part of this intensity contributed by random grains is assumed to be given by the quantity

$$\left(\frac{I_{hkl}}{I_{111}}\right)_{filings} (I_{111})_{specimen}$$

That portion of the total diffracted intensity due to the texture grains is then given by

$$(I_{hkl})_{specimen} - \left(\frac{I_{hkl}}{I_{111}}\right)_{filings} (I_{111})_{specimen}$$

Values of the relative volume of grains in the sheet for each texture were next computed as a function of the number of random grains by using the following relation:

$$\frac{\text{Texture grains}}{\text{Random grains}} = \frac{\left(\frac{I_{hkl}}{I_{111}}\right)_{\text{specimen}} - \left(\frac{I_{hkl}}{I_{111}}\right)_{\text{filings}}}{\left(\frac{I_{hkl}}{I_{111}}\right)_{\text{filings}}}$$

The values obtained as a result of these computations for the interior of the sheet are given in table 4. The surface was considered to be essentially the same as the interior, and, therefore, no additional calculations were necessary. (The results have also been expressed on a percentage basis. The values are given to the nearest 5 percent value.)

From the percentage values of table 4 the composition of the sheet was then determined. Where twin orientations occurred, the percentage values of table 4 were divided equally between the twin orientations. The complete makeup of the sheet is given in table 2.

APPENDIX B

METHOD OF COMPUTATION OF POISSON'S RATIO IN PLASTIC RANGE

Single Crystals

For single crystals of aluminum tested in tension, a knowledge of the orientation of the crystal with respect to the loading axis is sufficient to calculate relative values of plastic strain. When these strains are small, the effects of lattice rotation on the resultant deformation may be neglected. When these computations are made, it is necessary to transform the shear along a certain plane of the crystal in a certain direction into the resultant strain in any desired direction. This transformation can be conveniently made through the use of tensor transformation equations. The method of making these calculations is described subsequently.

The following system of coordinates is adopted:

(a) The 1-axis is normal to the slip plane which is of the $\{111\}$ type.

(b) The 2-axis is the slip direction of the <110> type in the slip plane.

(c) The 3-axis is normal to the plane determined by the 1- and 2-axes by using a right-hand convention.

It is desired to determine the strain in two orthogonal directions of the cross section when the single crystal is extended in the longitudinal direction. These orthogonal directions are designated as follows:

L	longitudinal direction of crystal
X	arbitrary direction in cross section of crystal
Y	direction in cross section perpendicular to L,X plane when a right-hand convention is used

The strain tensor for simple shear is given by

$$\epsilon_{mn} = \begin{pmatrix} 0 & \gamma_{12/2} & 0 \\ \gamma_{12/2} & 0 & 0 \\ 0 & 0 & 0 \end{pmatrix} = \begin{pmatrix} 0 & \epsilon_{12} & 0 \\ \epsilon_{12} & 0 & 0 \\ 0 & 0 & 0 \end{pmatrix}$$

where $\gamma_{12/2} = \epsilon_{12}$ designates the shear in the slip system.

By tensor transformation, the strain in the longitudinal direction is then given by

$$\epsilon_L = 2 l_{1L} l_{2L} \epsilon_{12}$$

and for the x- and y-directions by

$$\epsilon_x = 2 l_{1x} l_{2x} \epsilon_{12}$$

and

$$\epsilon_y = 2 l_{1y} l_{2y} \epsilon_{12}$$

where l_{1L} is the direction cosine between slip plane normal and longitudinal direction and l_{2L} is the direction cosine between slip direction and longitudinal direction. The symbols l_{1x}, l_{2x}, l_{1y}, and l_{2y} are similarly defined.

Values of Poisson's ratio for these directions are then given by

$$\mu_x = - \frac{\epsilon_x}{\epsilon_L} = - \frac{l_{1x} l_{2x}}{l_{1L} l_{2L}}$$

and

$$\mu_y = - \frac{\epsilon_y}{\epsilon_L} = - \frac{l_{1y} l_{2y}}{l_{1L} l_{2L}}$$

When the x- and y-directions correspond to thickness and width directions of a cross section, these expressions become

$$\mu_t = -\frac{\epsilon_t}{\epsilon_L} = -\frac{l_{1t}l_{2t}}{l_{1L}l_{2L}}$$

and

$$\mu_w = -\frac{\epsilon_w}{\epsilon_L} = -\frac{l_{1w}l_{2w}}{l_{1L}l_{2L}}$$

Before μ_t and μ_w can be computed, a knowledge of the orientation of the crystal is necessary. Once the orientation has been determined, the next step is to determine which of the 12 slip systems of the face-centered cubic crystal is operative, that is, which has the highest resolved shear stress for the given orientation. This information is obtained from figure 15(a) which is a stereographic projection showing the slip systems of a face-centered cubic crystal. Within each of the triangles a combination of slip plane and slip system is listed. When the specimen axis is plotted in figure 15(a), the appropriate slip system is defined and the required angles may be either computed or measured by using a Wulff net.

In many instances more than one slip system is active. This condition occurs whenever the specimen axis lies on a boundary between triangular areas, and the value plotted is the average of the values determined for each slip system. In one case, that is, where the specimen axis is in the [100] direction, eight slip systems are equally loaded; whereas in some other cases, four or six slip systems must be considered. Based on these relationships, the curve of figure 14 and the series of curves of figure 16 have been computed. These curves give the values of μ_w for single crystals possessing the same orientation with respect to the rolling direction as the ideal orientations of the 3S-O material.

The values of the maximum and minimum strains in the cross section are obtained as follows: The 1, 2, 3 axes are defined as before, but let the x-axis be fixed in the slip plane at a right angle to the projection of the specimen axis on the slip plane. The y-axis is then perpendicular to the other two axes. Let these axes be called the 1', 2', 3' axes. These axes are shown in figure 20(a).

The strains in this system are given by the following set of equations:

$$\epsilon_{1'1'} = (\cos \lambda \cos \beta)\gamma_{12}$$

$$\epsilon_{2'2'} = -(\cos \lambda \cos \beta)\gamma_{12}$$

$$\epsilon_{3'3'} = 0$$

$$\epsilon_{1'2'} = \epsilon_{2'1'} = (\cos^2\lambda \cos \varphi - \cos \beta \sin \lambda)\gamma_{12/2}$$

$$\epsilon_{1'3'} = \epsilon_{3'1'} = (\cos \lambda \sin \varphi)\gamma_{12/2}$$

$$\epsilon_{2'3'} = \epsilon_{3'2'} = (-\sin \lambda \sin \varphi)\gamma_{12/2}$$

where λ is the angle between the specimen axis and the normal to the slip plane, β is the angle between the specimen axis and the slip direction, and φ is the angle between the slip direction and the projection of the specimen axes on the slip plane.

In order to compute the maximum and minimum values of strain in the cross section, consider the system of coordinates shown in figure 20(b). The strain in any direction of the cross section may be determined by using tensor transformation equations. For the arbitrary directions 2" and 3" rotated by an angle α in the cross section from the 1', 2', 3' axes system, these strains are

$$\epsilon_{2"2"} = \epsilon_{2'2'} \cos^2\alpha + \epsilon_{2'3'} \sin 2\alpha$$

$$\epsilon_{3"3"} = \epsilon_{2'2'} \cos^2\alpha - \epsilon_{2'3'} \sin 2\alpha$$

If the derivative of these expressions is taken with respect to α and then set equal to zero, the maximum and minimum values of strain are found to occur at a value of α given by

$$\tan 2\alpha = \frac{\sin \Phi}{\cos \beta} \tan \lambda$$

or

$$\tan 2\alpha = \frac{\sqrt{\sin^2\lambda - \cos^2\beta}}{\cos \beta \cos \lambda}$$

Then, by solving for the values of maximum and minimum strain,

$$\epsilon_{2"2"} = -\frac{\gamma}{2} \cos(\lambda - \beta)$$

$$\epsilon_{3"3"} = -\frac{\gamma}{2} \cos(\lambda + \beta)$$

The values of Poisson's ratio corresponding to these strains are

$$\frac{\epsilon_{2"2"}}{\epsilon_{1'1'}} = \frac{1}{2}(1 + \tan \lambda \tan \beta)$$

$$\frac{\epsilon_{3"3"}}{\epsilon_{1'1'}} = -\frac{1}{2}(1 - \tan \lambda \tan \beta)$$

Polycrystalline Aggregates

The values of Poisson's ratios for a polycrystalline aggregate may be computed on the basis of single-crystal behavior for the 3S-O material. When the calculations are made, the following conditions are assumed:

(1) The longitudinal strain in each grain is the same as that for the aggregate as a whole.

(2) The grains have been extended far enough so that all the grains have slipped.

(3) The transverse strain in the aggregate is the average of the transverse strains of the individual grains.

(4) The elastic contribution to lateral strain is negligible.

Inasmuch as the Poisson's ratio for each ideal orientation has already been computed, it is necessary only to weight each value for a given orientation in accordance with the percentage of each present as given in table 2. The results of this calculation are shown in figure 17(a) which has been obtained by fairing a smooth curve to remove the discontinuities of the theoretical curve. The experimental results are also plotted in figure 18 for comparison with the theoretical curve.

REFERENCES

1. Klingler, L. J., and Sachs, G.: Dependence of the Stress-Strain Curves of Cold-Worked Metals Upon the Testing Direction. Jour. Aero. Sci., vol. 15, no. 3, Mar. 1948, pp. 151-154.

2. Klingler, L. J., and Sachs, G.: Plastic Flow Characteristics of Aluminum-Alloy Plate. Jour. Aero. Sci., vol. 15, no. 10, Oct. 1948, pp. 599-604.

3. Klingler, L. J., and Sachs, G.: Fracturing Characteristics of Aluminum-Alloy Plate. Jour. Aero. Sci., vol. 15, no. 12, Dec. 1948, pp. 731-734.

4. Anon.: Alcoa Aluminum and Its Alloys. Aluminum Co. of America, 1950.

5. Kotanchik, Joseph N., Woods, Walter, and Weinberger, Robert A.: Investigation of Methods of Supporting Single-Thickness Specimens in a Fixture for Determination of Compressive Stress-Strain Curves. NACA WR L-189, 1945. (Formerly NACA RB L5E15.)

6. Baldwin, William M., Jr., Howald, T. S., and Ross, A. W.: Relative Triaxial Deformation Rates. Tech. Pub. No. 1808, Trans. Am. Inst. Mining and Metallurgical Eng., vol. 166, 1946, pp. 86-109.

7. V. Göler, and Sachs, G.: Das Verhalten von Aluminiumkristallen bei Zugversuchen. I. Geometrische Grundlagen. Zeitschr f. Physik, vol. 41, no. 2/3, Feb. 10, 1927, pp. 103-115.

8. Karnop, R., and Sachs, G.: Das Verhalten von Aluminiumkristallen bei Zugversuchen. II. Experimenteller Teil. Zeitschr. f. Physik, vol. 41, no. 2/3, Feb. 10, 1927, pp. 116-139.

9. Hedgepeth, John M., Batdorf, S. B., and Sanders, J. Lyell, Jr.: On the Angular Distribution of Slip Lines in Polycrystalline Aluminum Alloy. NACA TN 2577, 1951.

10. Barrett, Charles S.: Structure of Metals. Second ed., McGraw-Hill Book Co., Inc., 1952.

11. Beck, Paul A., and Hu, Hsun: Annealing Textures in Rolled Face-Centered Cubic Metals. Jour. Metals, vol. 4, no. 1, sec. 1, Jan. 1952, pp. 83-90.

12. Taylor, A.: An Introduction to X-ray Metallography. John Wiley & Sons, Inc., 1945, p. 363.

TABLE 1.- MECHANICAL PROPERTIES OF 3S-0 ALUMINUM ALLOY

Prestrain, percent	Angle between rolling direction and specimen axis, deg	Tensile yield stress, psi; 0.2 percent offset	Compressive yield stress, psi; 0.2 percent offset	Ultimate tensile strength, psi
0	0	5,520	6,170	16,210
	30	5,670	6,030	15,750
	45	5,600	5,930	15,440
	60	5,680	5,840	15,300
	90	5,730	5,750	15,710
1	0	9,250	7,630	16,450
	30	8,780	8,220	15,960
	45	8,700	8,790	15,530
	60	8,560	8,970	15,440
	90	8,510	9,260	15,780
5	0	12,830	11,050	17,010
	30	12,500	12,160	15,920
	45	12,500	12,560	15,690
	60	12,350	12,860	14,400
	90	12,110	13,010	15,260

TABLE 2.- COMPOSITION OF 3S-0 ALUMINUM-ALLOY SHEET

Ideal orientation		Percentage
(001)[100]		35
(110)[1$\bar{1}$2]	twin orientations	7.5
(110)[$\bar{1}$12]	twin orientations	7.5
(112)[$\bar{1}\bar{1}$1]		10
(113)[$\bar{1}\bar{2}$1]	twin orientations	2.5
($\bar{2}\bar{1}$1)[113]	twin orientations	2.5
(210)[$\bar{1}$22]	twin orientations	10
(210)[1$\bar{2}$2]	twin orientations	10
Random		15

TABLE 3.- RELATIVE INTENSITY $\left(I_{hkl}/I_{lll}\right)_{filings}$ FOR RANDOMLY ORIENTED GRAINS

Reflection	Experiment	Theory
111	1.00	1.000
200	.47	.474
220	.27	.274
311	.30	.294
222	.08	.082
400	.03	.037
331	.13	.124
420	.13	.124
422	.13	.140
511	----	.328
333	----	.109

TABLE 4.- RELATIVE PROPORTION OF TEXTURE GRAINS TO RANDOM GRAINS

Plane	Ratio of texture grains to random grains	Percentage
(001)	2.3	35
(110)	1.0	15
(112)	.6	10
(113)	.3	5
(210)	1.3	20
Random	1.0	15

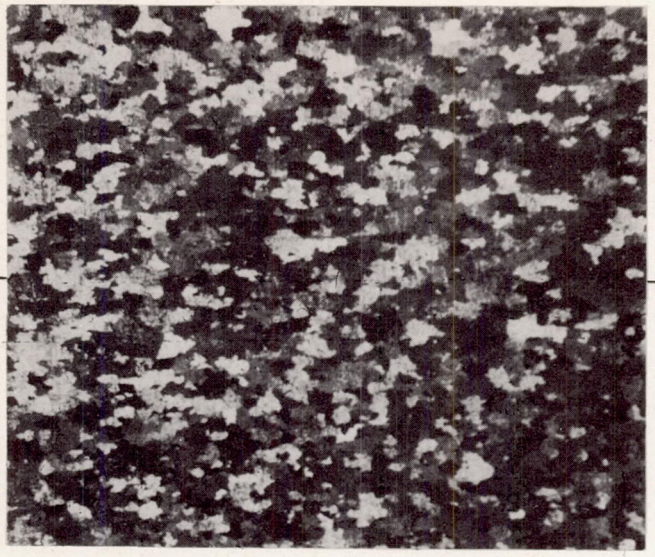

(a) Section parallel to rolling plane. Lines indicate rolling direction.

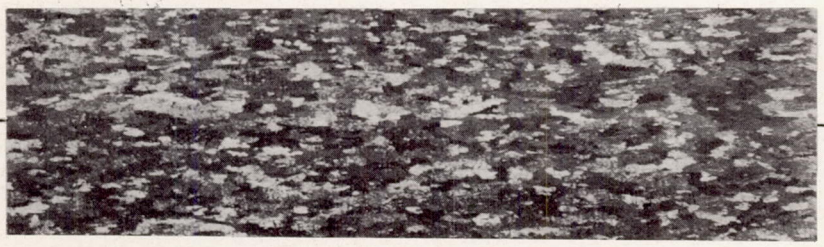

(b) Section perpendicular to transverse direction. Lines indicate rolling direction.

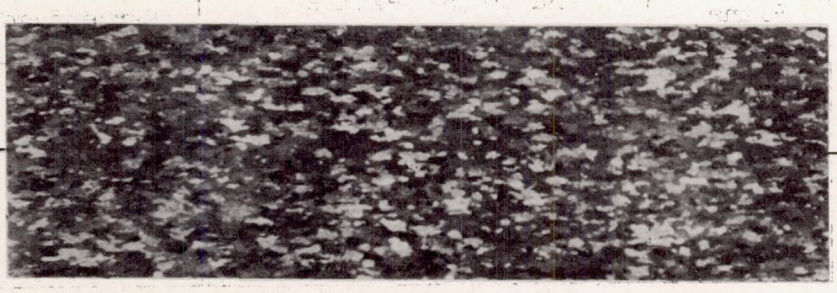

L-85620

(c) Section perpendicular to rolling direction. Lines indicate transverse direction.

Figure 1.- Photomicrographs of 3S-0 aluminum alloy. X12.

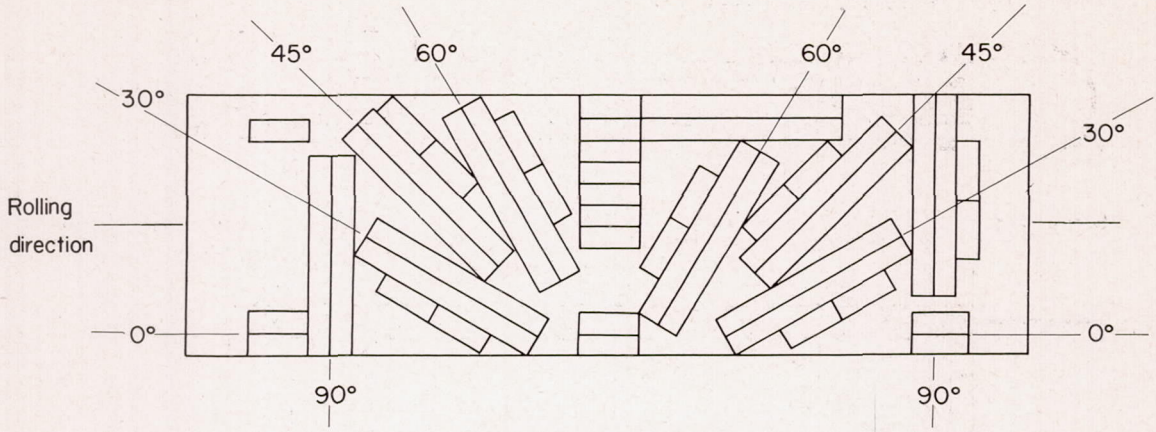

(a) Specimen layout.

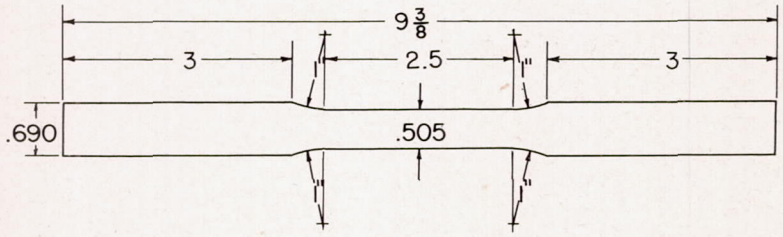

(b) Standard tension specimen.

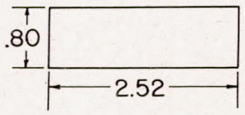

(c) Standard compression specimen.

Figure 2.- Specimen layout and dimensions for standard tension and compression specimens.

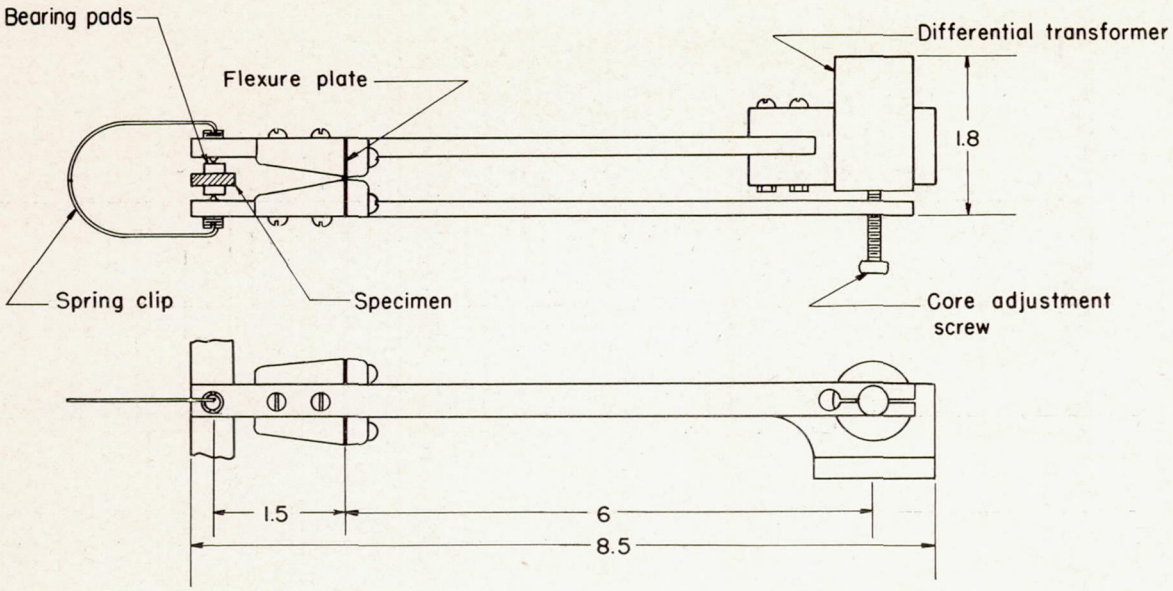

(a) Thickness gage.

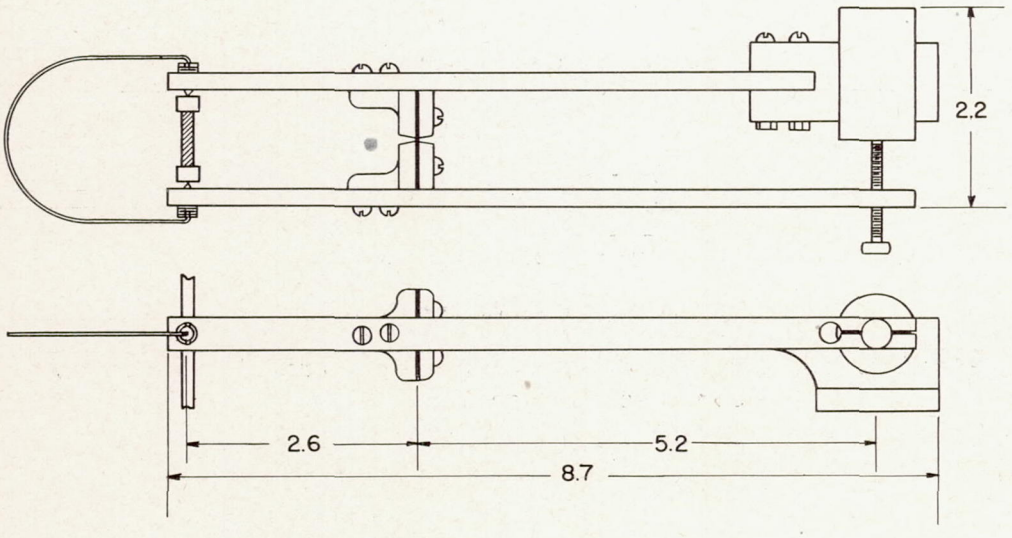

(b) Width gage.

Figure 3.- Schematic diagram of lateral strain gages.

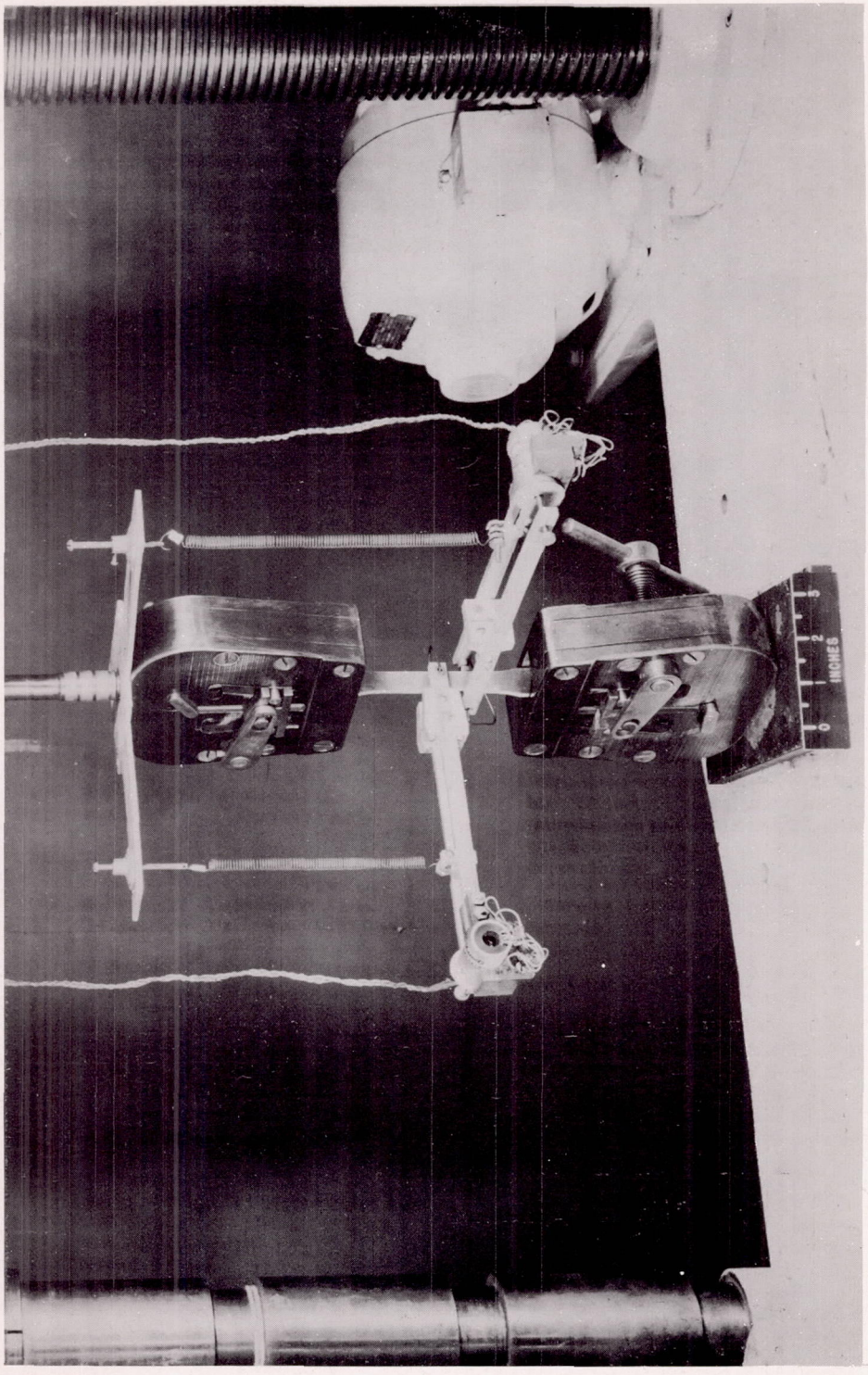

L-67700

Figure 4.- Transverse gages mounted for test.

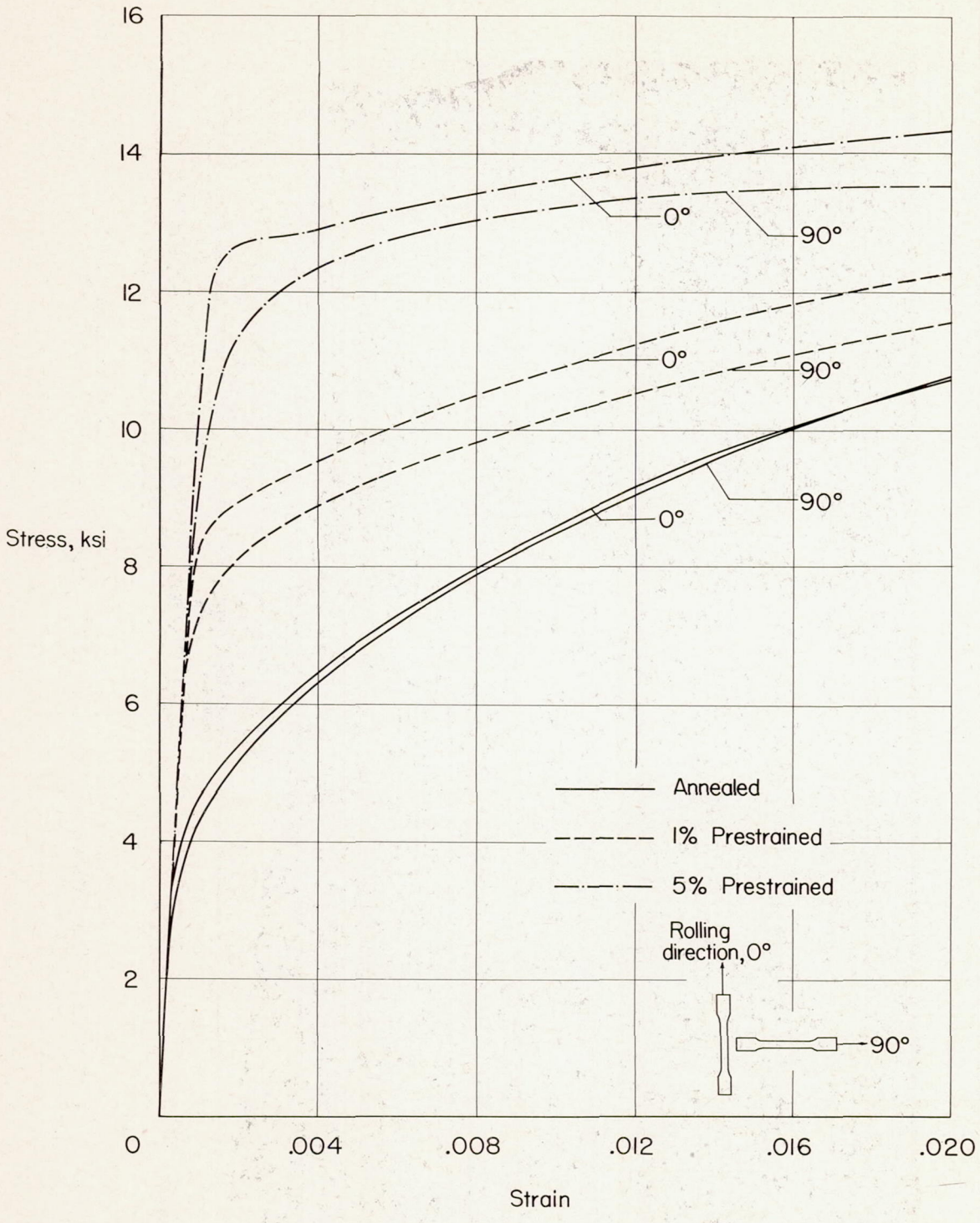

Figure 5.- Longitudinal and transverse tensile stress-strain curves of 3S aluminum alloy at various amounts of prestrain.

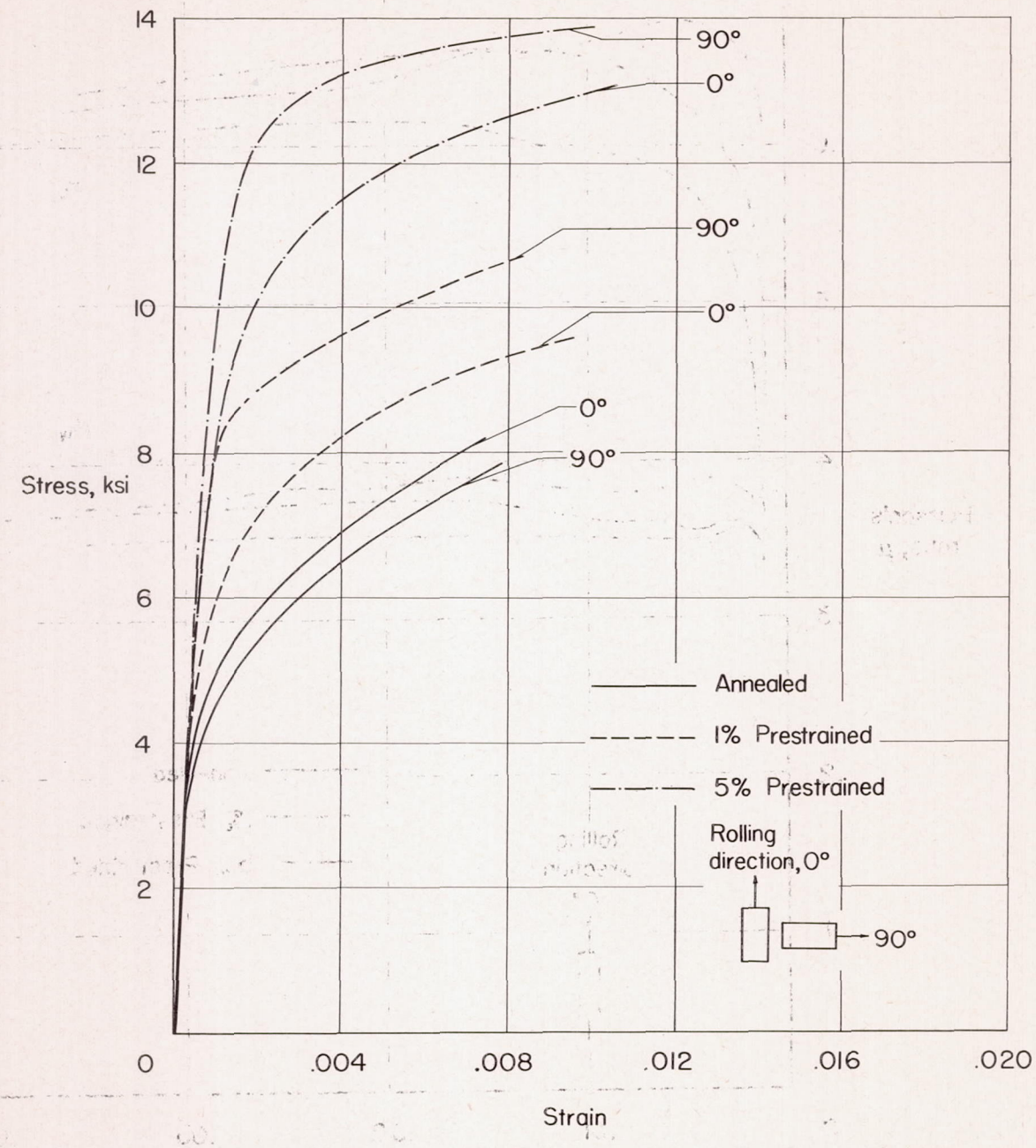

Figure 6.- Longitudinal and transverse compressive stress-strain curves of 3S aluminum alloy at various amounts of prestrain.

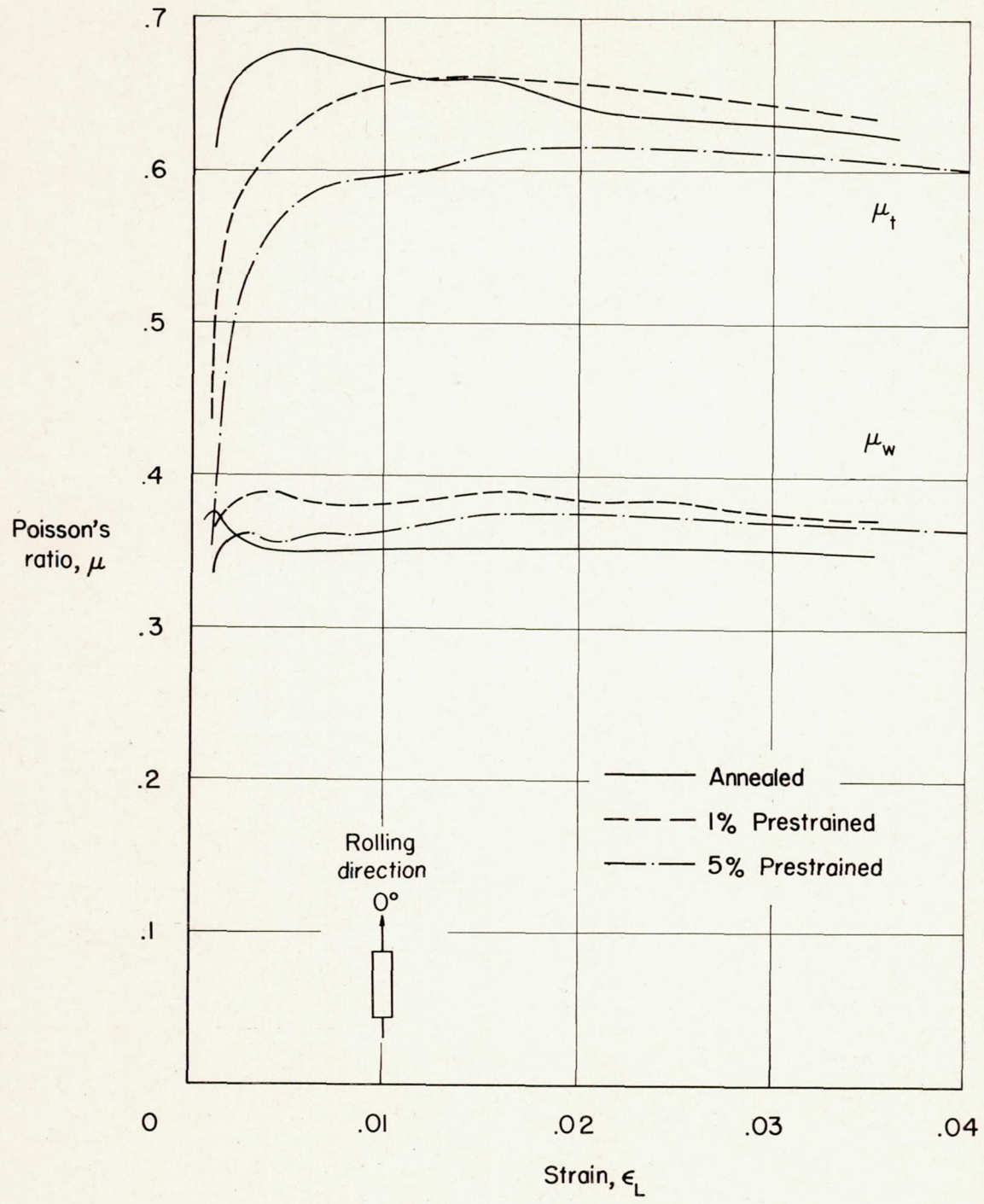

Figure 7.- Variation of Poisson's ratio with longitudinal strain in both width and thickness directions. Specimen axis is in rolling direction.

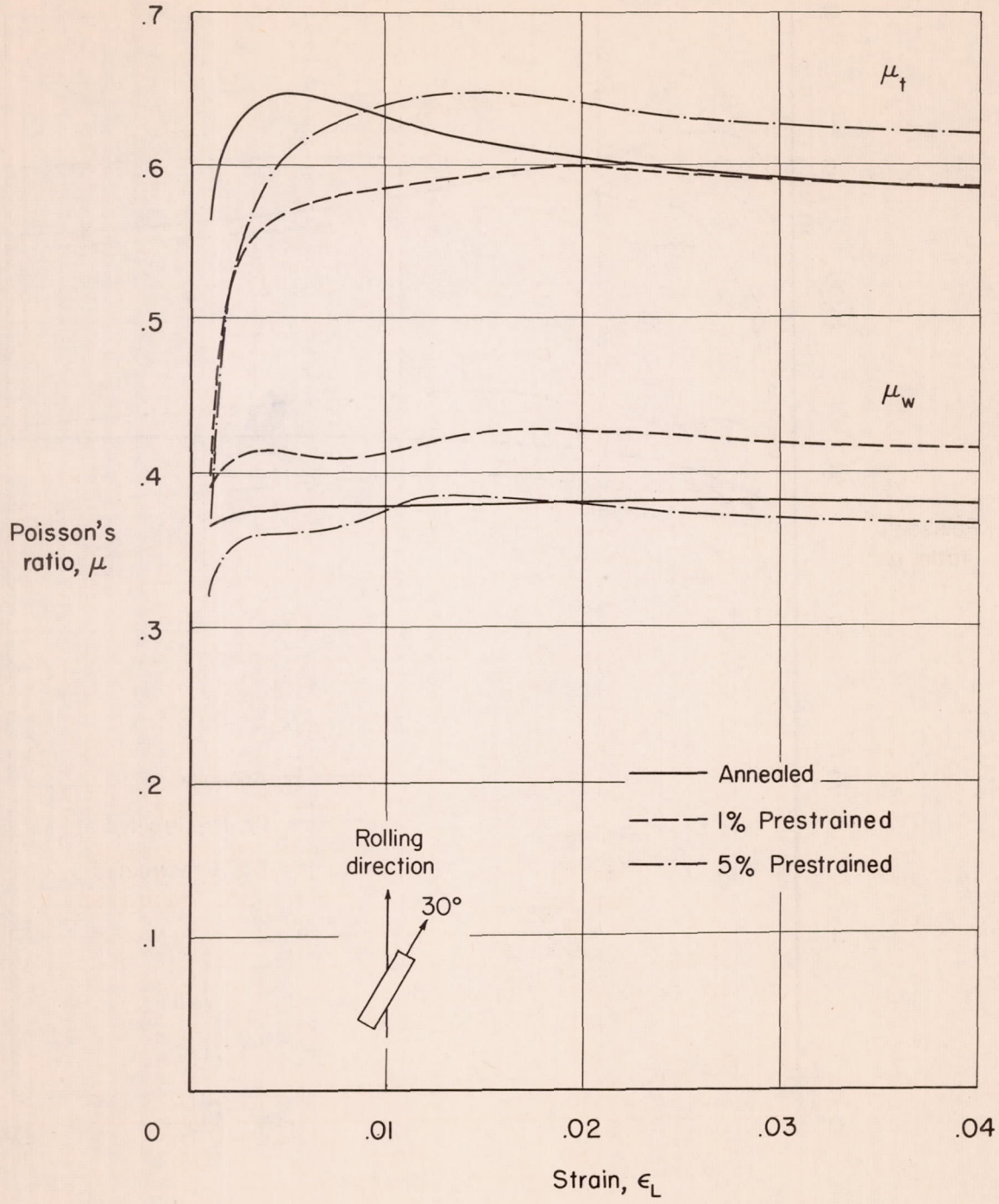

Figure 8.- Variation of Poisson's ratio with longitudinal strain in both width and thickness directions. Specimen axis is 30° to rolling direction.

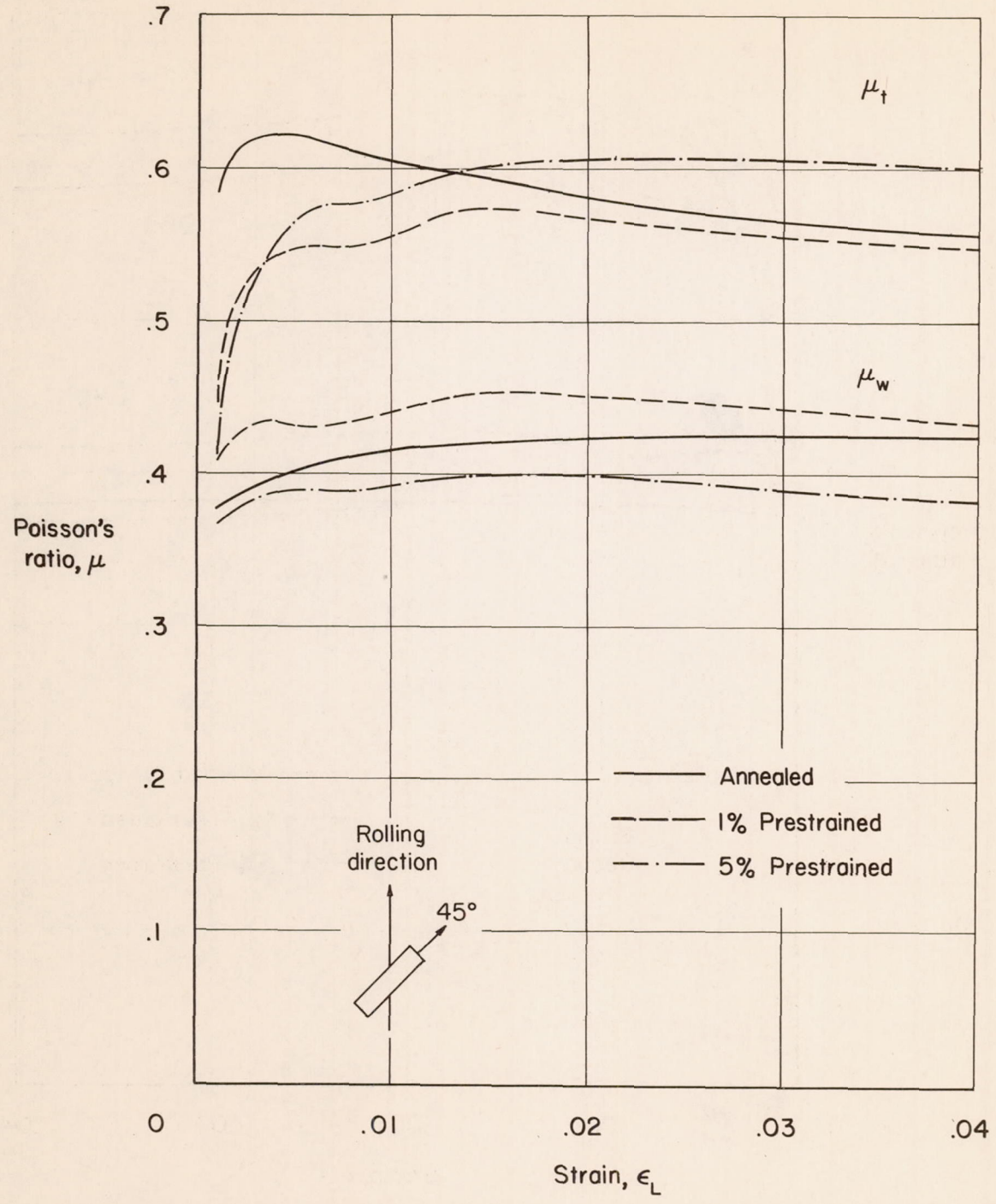

Figure 9.- Variation of Poisson's ratio with longitudinal strain in both width and thickness directions. Specimen axis is 45° to rolling direction.

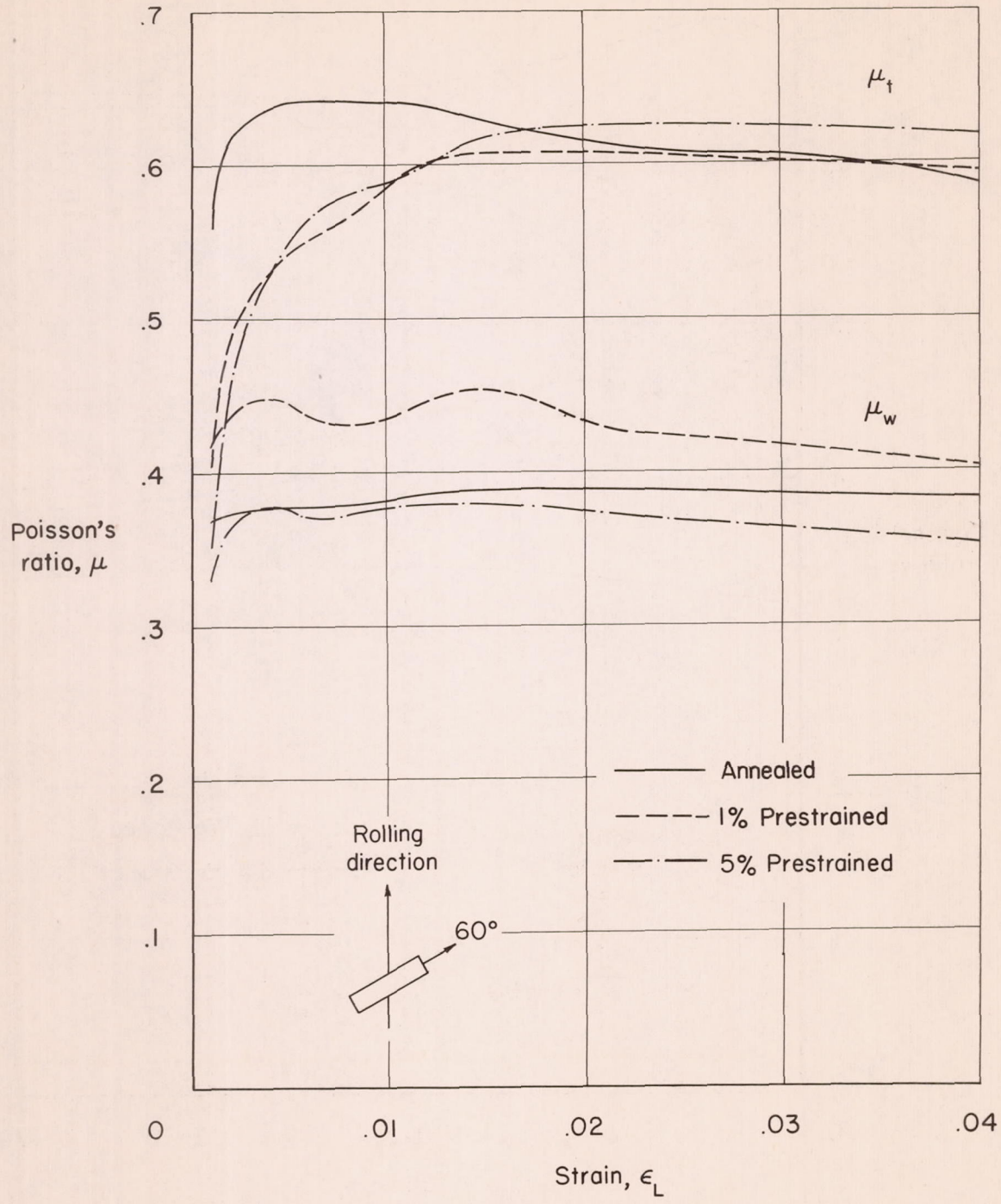

Figure 10.- Variation of Poisson's ratio with longitudinal strain in both width and thickness directions. Specimen axis is 60° to rolling direction.

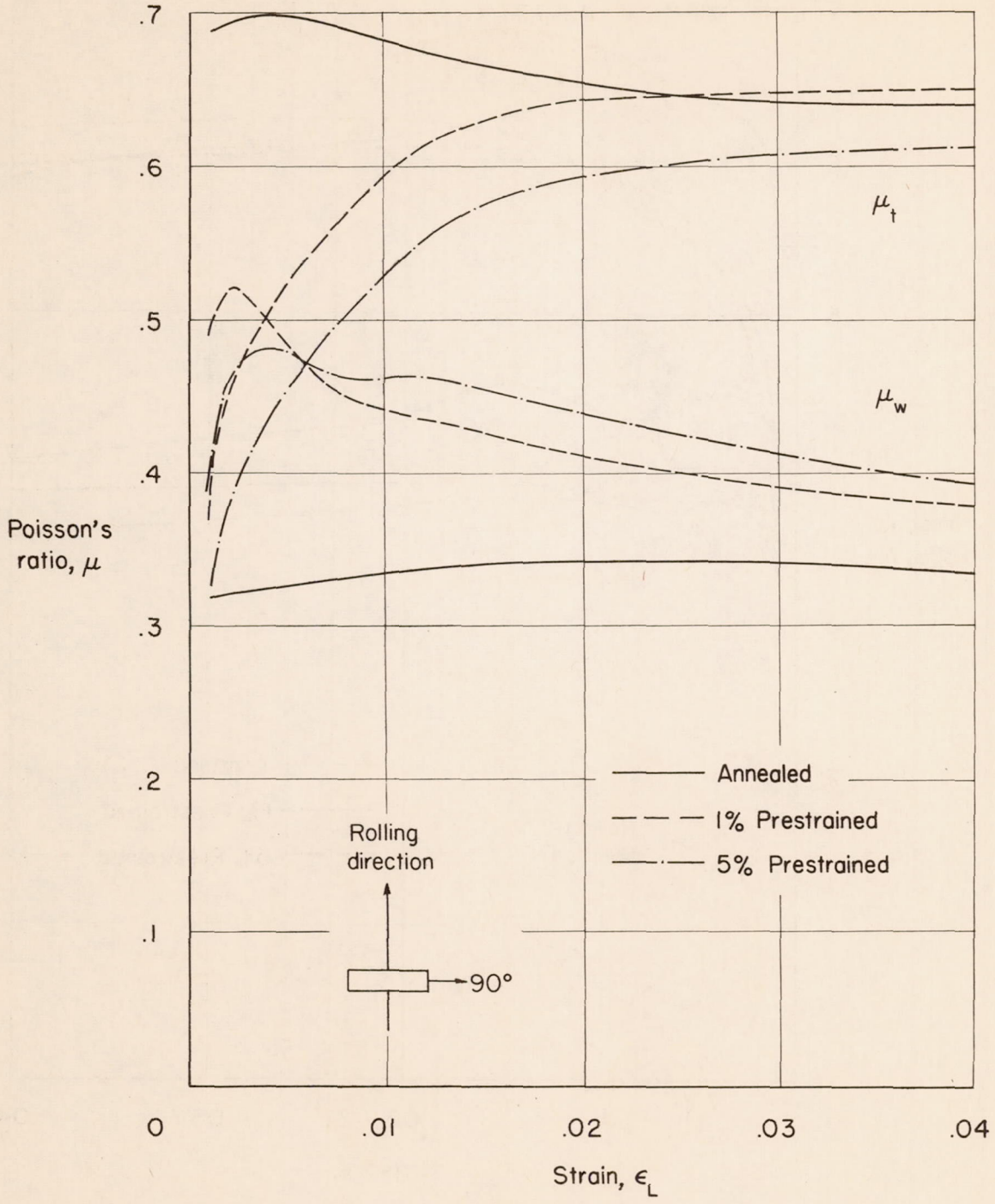

Figure 11.- Variation of Poisson's ratio with longitudinal strain in both width and thickness directions. Specimen axis is 90° to rolling direction.

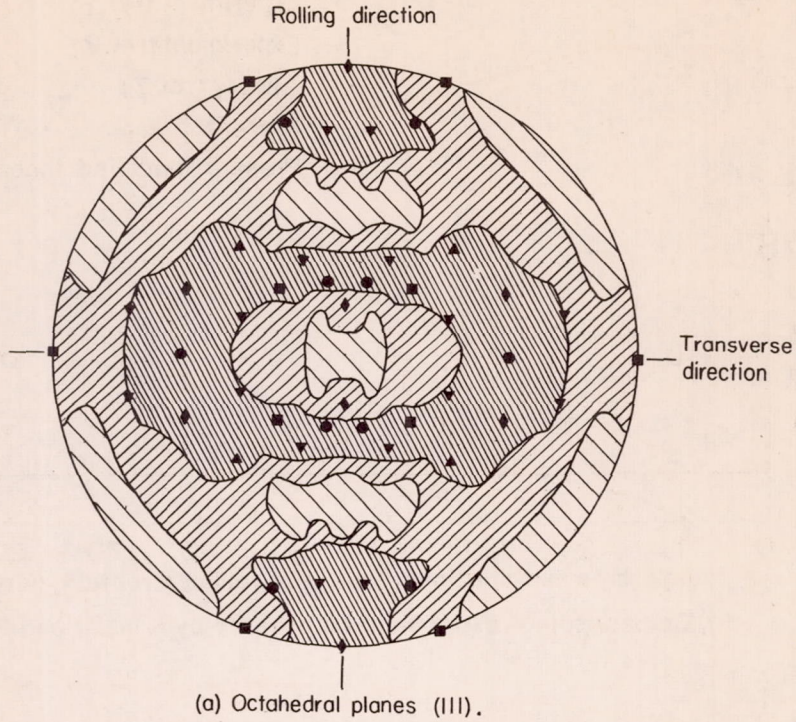

(a) Octahedral planes (111).

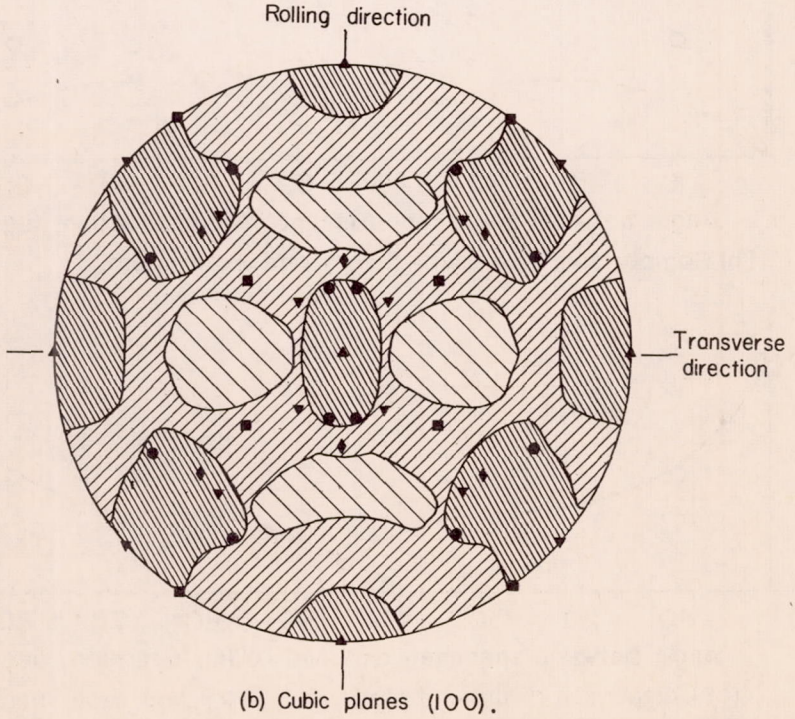

(b) Cubic planes (100).

Figure 12.- Pole figures for interior of 3S-0 aluminum alloy. Ideal orientations are indicated as follows: ▲, (100)[001]; ■, (110)[112]; ⬬, (113)[211]; ⬬, (112)[111]; and ▼, (210)[122].

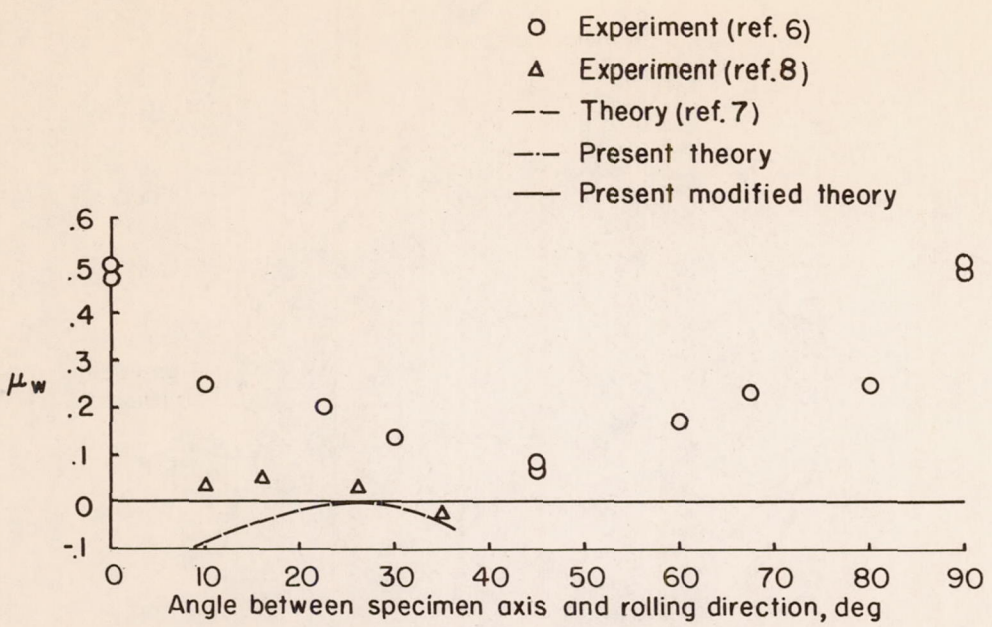

(a) Comparison of experiment and theory by Klingler and Sachs.

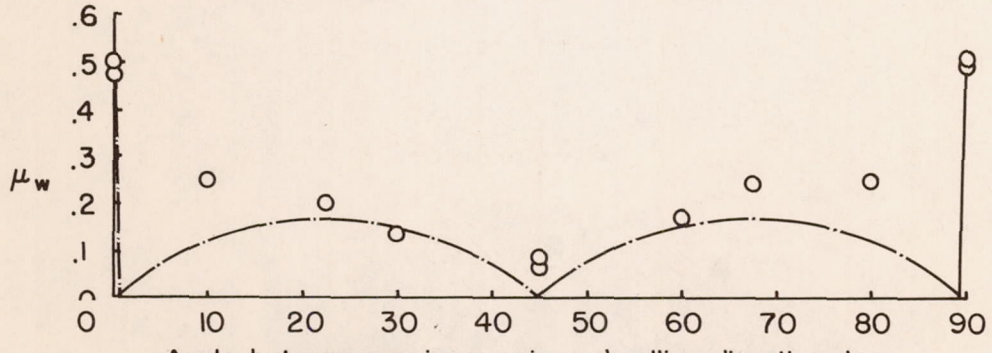

(b) Comparison of present theory and experiment.

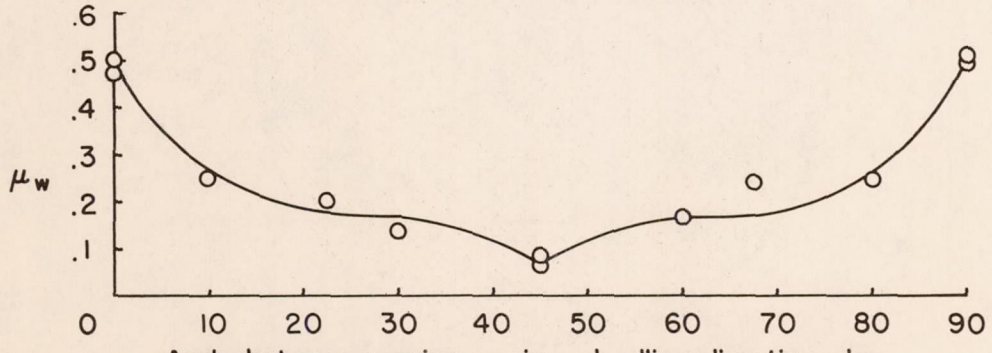

(c) Comparison of present modified theory and experiment.

Figure 13.- Variation of Poisson's ratio in width direction for cubically alined copper.

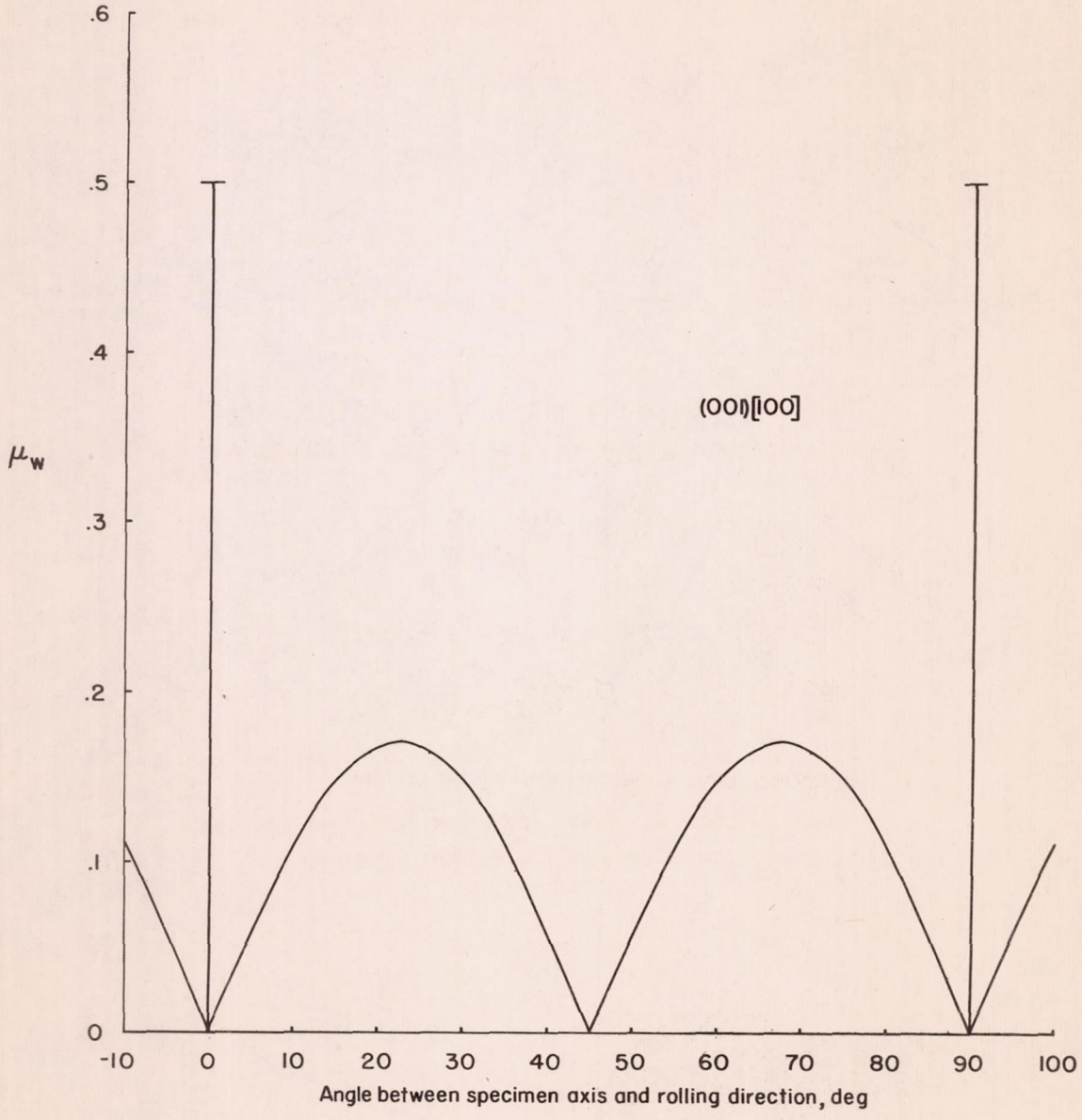

Figure 14.- Variation of Poisson's ratio in width direction for cubically alined face-centered cubic crystal.

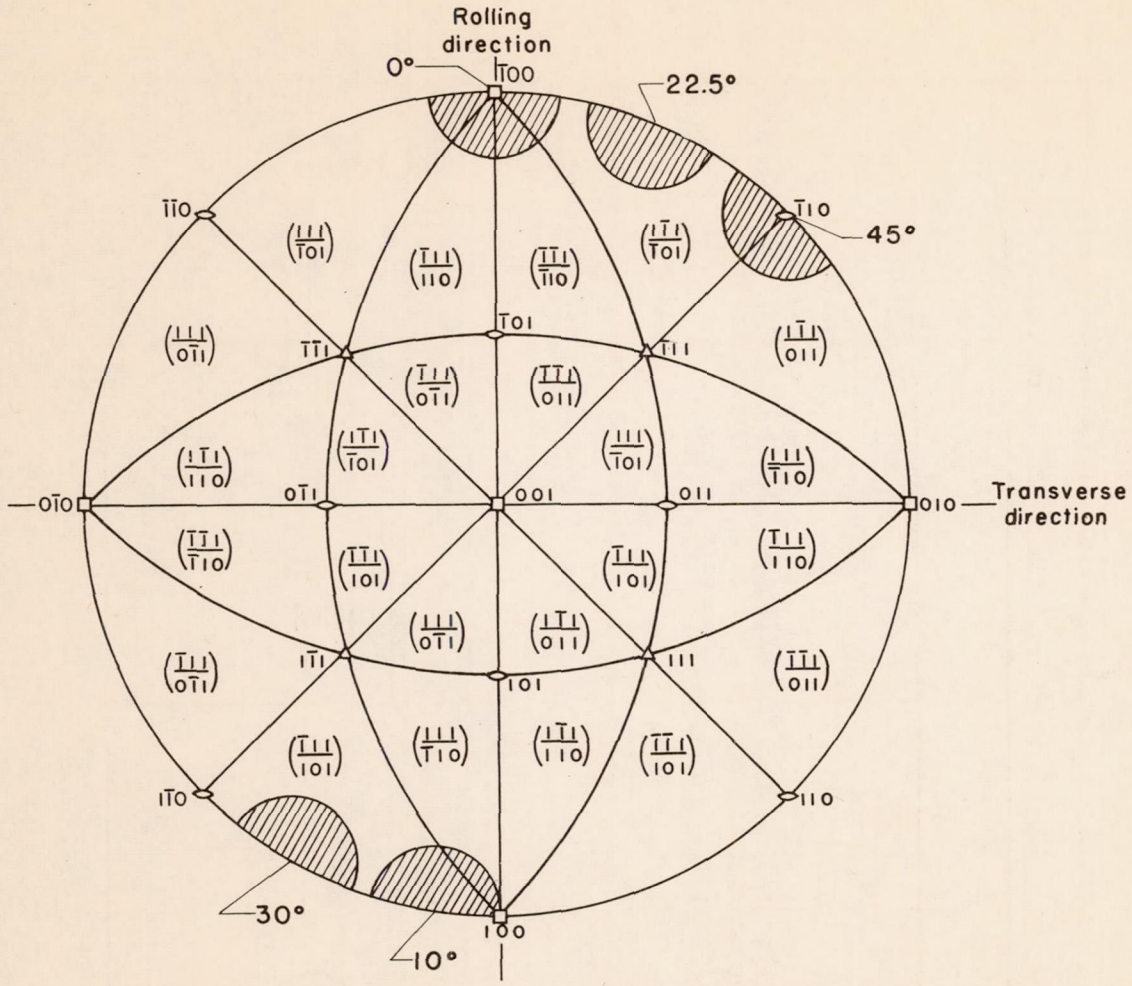

(a) Stereographic projection showing slip systems.

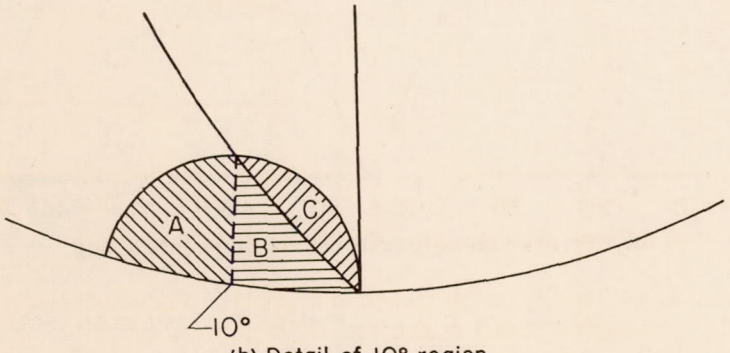

(b) Detail of 10° region.

Figure 15.- Stereographic projection of face-centered cubic crystal indicating slip systems. Shaded regions indicate spread about ideal orientation present in cubically alined copper.

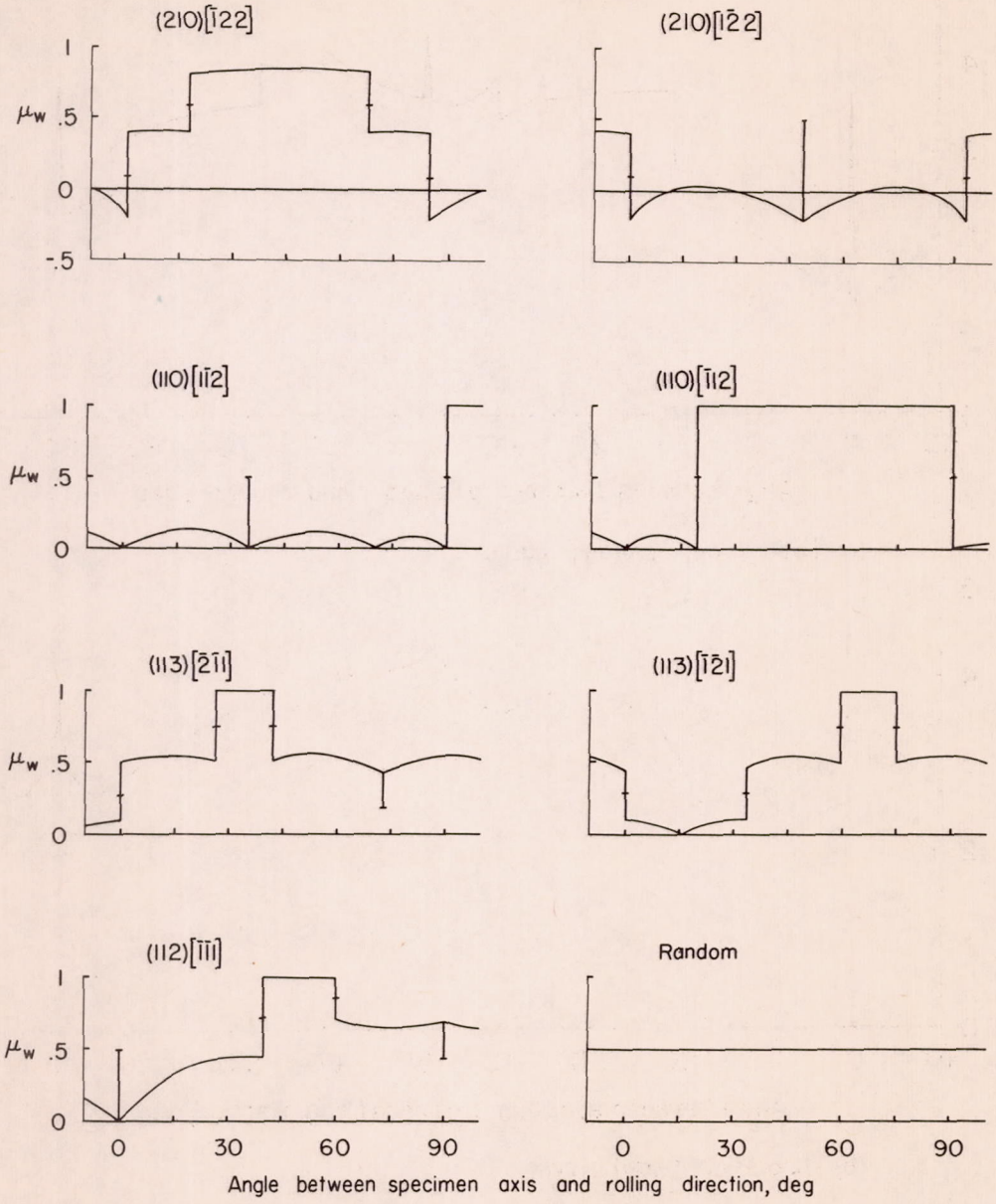

Figure 16.- Variation of Poisson's ratio in width direction for face-centered cubic single crystals.

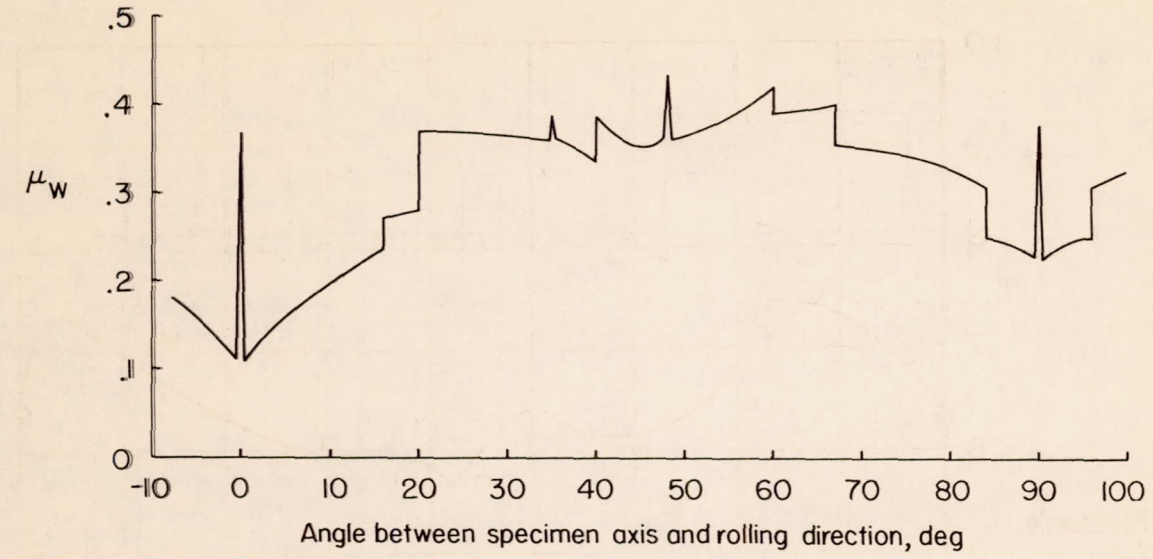

(a) Theoretical average curve.

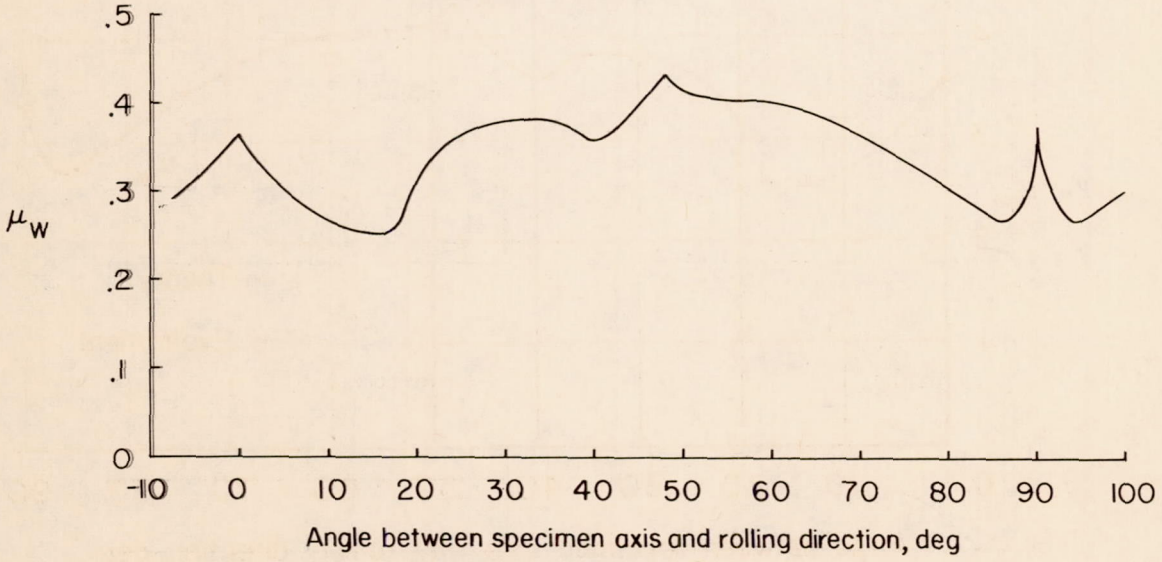

(b) Theoretical faired curve.

Figure 17.- Theoretical and faired curves for Poisson's ratio in width direction for 3S-0 aluminum-alloy sheet.

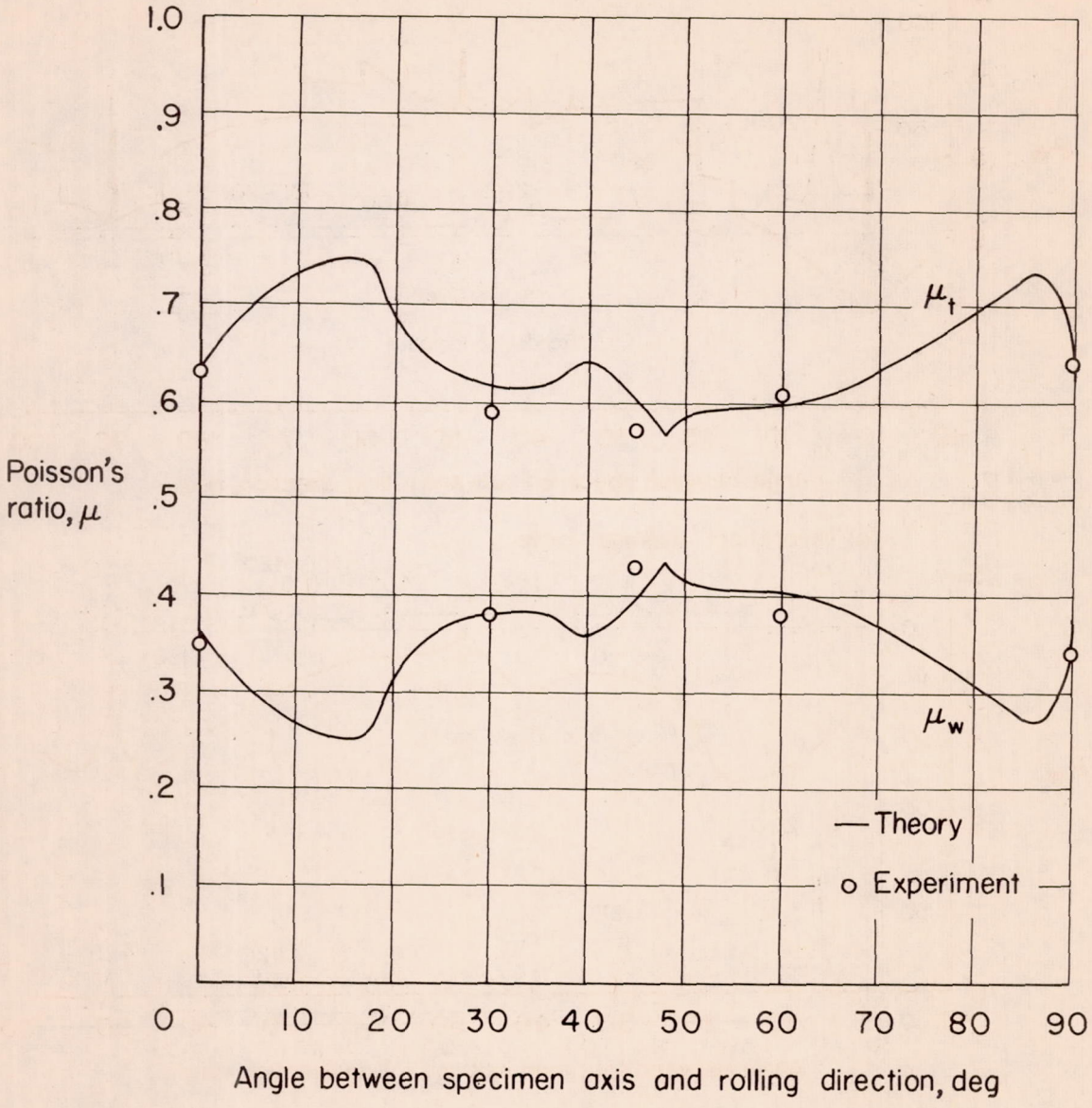

Figure 18.- Comparison of experimental and theoretical values of Poisson's ratio for 3S-0 aluminum-alloy sheet.

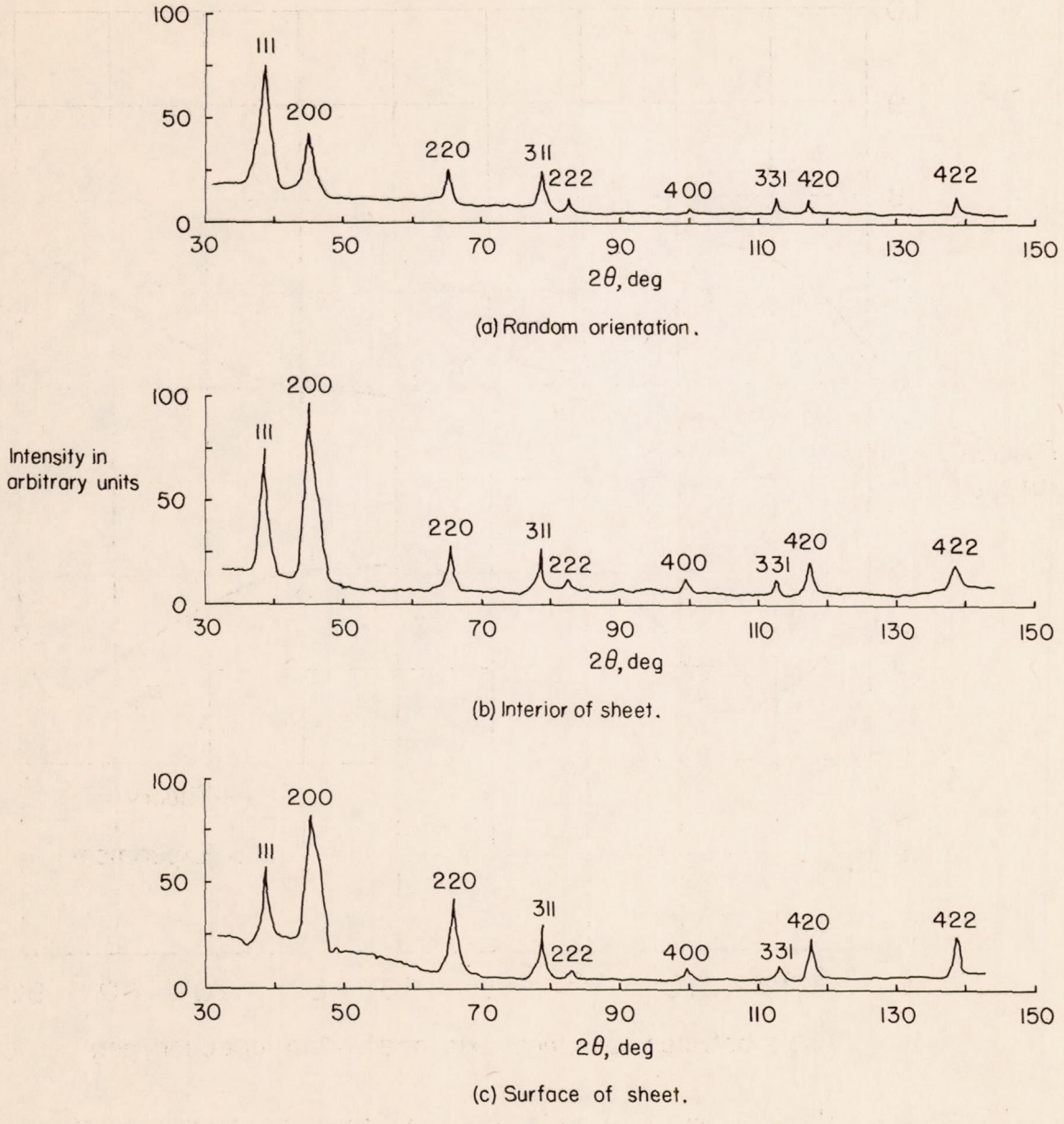

Figure 19.- Representative spectrometer charts from 3S-0 aluminum-alloy sheet. Copper Kα radiation.

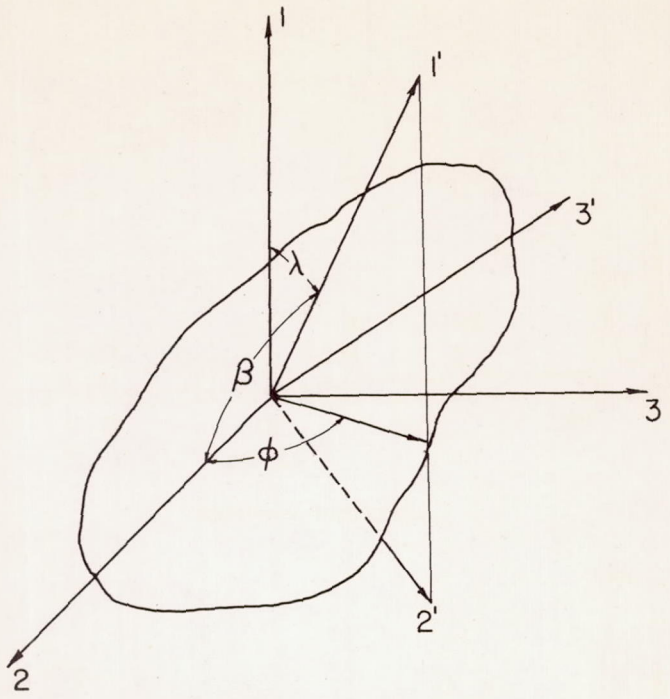

(a) Coordinate axes.

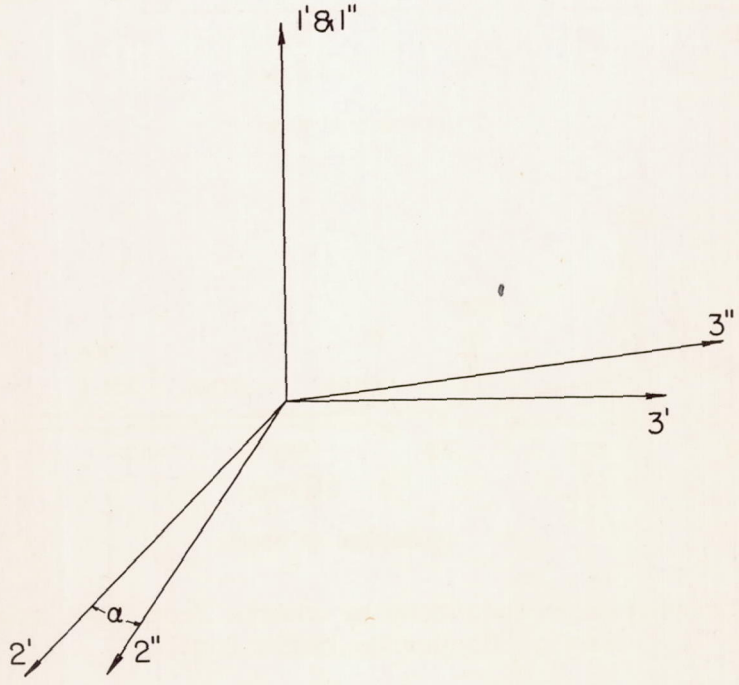

(b) Rotation about 1' axis.

Figure 20.- Geometry of planes, directions, and angles involved in the analysis.